AD-A132 893 STATE-OF-THE-ART FOR ASSESSING EARTHQUAKE HAZARDS IN THE UNITED STATES RE..(U) CALIFORNIA UNIV BERKELEY B A BOLT AUG 83 WES-MP-S-73-1-20 DACW39-82-M-1125 1/2

UNCLASSIFIED F/G 8/11 NL

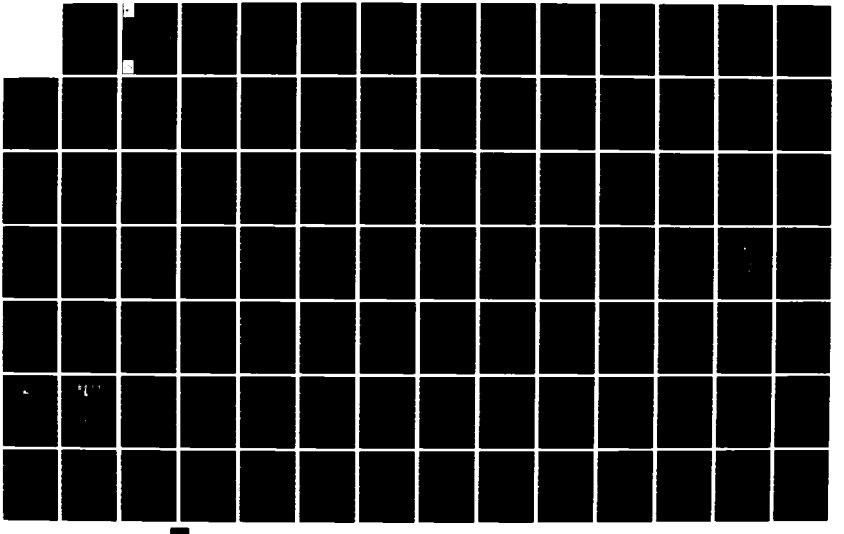

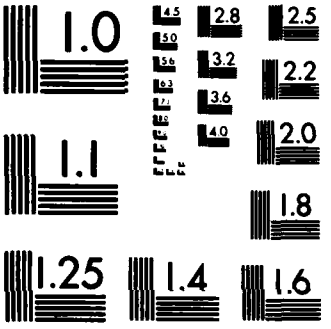

US Army Corps of Engineers

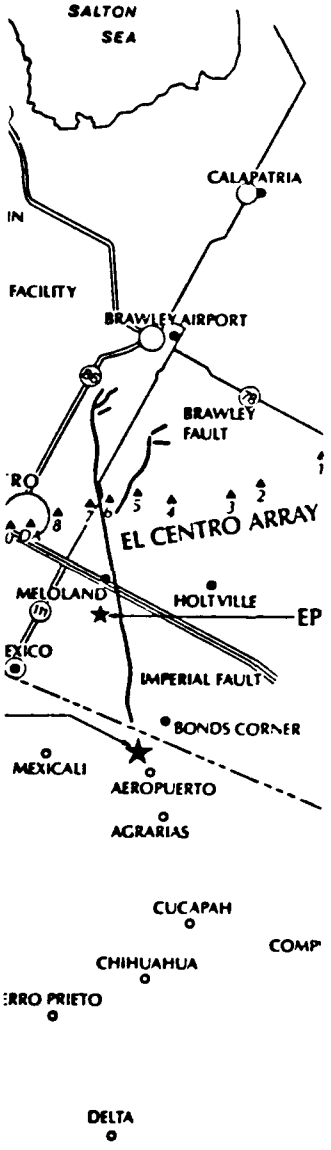

GEOTECHNICAL LABORATORY

(1)

MISCELLANEOUS PAPER S-73-1

STATE-OF-THE-ART FOR ASSESSING EARTHQUAKE HAZARDS IN THE UNITED STATES

Report 20

THE CONTRIBUTION OF DIRECTIVITY FOCUSING TO EARTHQUAKE INTENSITIES

by

Bruce A. Bolt

University of California
Berkeley, Calif. 94720

August 1983

Report 20 of a Series

Prepared for Office, Chief of Engineers, U. S. Army
Washington, D. C. 20314

Under Contract No. DACW39-82-M-1125

Monitored by Geotechnical Laboratory
U. S. Army Engineer Waterways Experiment Station
P. O. Box 631, Vicksburg, Miss. 39180

When this report is no longer needed return it to the originator.

The findings in this report are not to be construed as an official Department of the Army position unless so designated by other authorized documents.

The contents of this report are not to be used for advertising, publication, or promotional purposes. Citation of trade names does not constitute an official endorsement or approval of the use of such commercial products.

The covers of U. S. Army Engineer Waterways Experiment Station (WES) engineering and scientific reports have been redesigned. Each WES Laboratory and support organization will have its own distinctive color imprinted on white coverstock. This standardizes WES publications and enhances their professional appearance.

Unclassified

SECURITY CLASSIFICATION OF THIS PAGE (When Data Entered)

REPORT DOCUMENTATION PAGE	READ INSTRUCTIONS BEFORE COMPLETING FORM
1. REPORT NUMBER: Miscellaneous Paper S-73-1-20	2. GOVT ACCESSION NO.: AD-A132 893
	3. RECIPIENT'S CATALOG NUMBER:
4. TITLE (and Subtitle): STATE-OF-THE-ART FOR ASSESSING EARTHQUAKE HAZARDS IN THE UNITED STATES; Report 20, THE CONTRIBUTION OF DIRECTIVITY FOCUSING TO EARTHQUAKE INTENSITIES	5. TYPE OF REPORT & PERIOD COVERED: Report 20 of a series
	6. PERFORMING ORG. REPORT NUMBER:
7. AUTHOR(s): Bruce A. Bolt	8. CONTRACT OR GRANT NUMBER(s): Contract No. DACW 39-82-M-1125
9. PERFORMING ORGANIZATION NAME AND ADDRESS: University of California, Berkeley, Calif. 94720	10. PROGRAM ELEMENT, PROJECT, TASK AREA & WORK UNIT NUMBERS:
11. CONTROLLING OFFICE NAME AND ADDRESS: Office, Chief of Engineers, U. S. Army, Washington, D. C. 20314	12. REPORT DATE: August 1983
	13. NUMBER OF PAGES: 93
14. MONITORING AGENCY NAME & ADDRESS (if different from Controlling Office): U. S. Army Engineer Waterways Experiment Station, Geotechnical Laboratory, P. O. Box 631, Vicksburg, Miss. 39180	15. SECURITY CLASS. (of this report): Unclassified
	15a. DECLASSIFICATION/DOWNGRADING SCHEDULE:

16. DISTRIBUTION STATEMENT (of this Report)

Approved for public release; distribution unlimited.

17. DISTRIBUTION STATEMENT (of the abstract entered in Block 20, if different from Report)

18. SUPPLEMENTARY NOTES

Available from National Technical Information Service, 5285 Port Royal Road, Springfield, Va. 22161.

19. KEY WORDS (Continue on reverse side if necessary and identify by block number)

Earthquake engineering
Earthquakes
Ground motion
Seismology

20. ABSTRACT (Continue on reverse side if necessary and identify by block number)

This report describes available evidence for effects of moving sources in earthquakes and analyzes them in terms of the physics of wave emission. The study is addressed mainly to questions arising in geotechnical investigations for engineering purposes and suggestions are made on the significance of the effect in strong ground motion estimation.

From a seismological point of view, the effect of the moving source has

(Continued)

DD FORM 1 JAN 73 1473 EDITION OF 1 NOV 65 IS OBSOLETE

Unclassified

SECURITY CLASSIFICATION OF THIS PAGE (When Data Entered)

20. ABSTRACT (Continued).

been clearly demonstrated in numerous studies using seismographs located at both moderate and great distances (i.e., the far field) from the source. Such studies, however, usually concern long-period seismic waves with periods above 2 to 5 seconds. Second, when seismic waves in the near field with a range of wave frequencies characteristic of engineered structures (i.e., 1 Hz to 10 Hz) are considered, there is as yet only limited definitive evidence available, and this is somewhat contradictory. Nevertheless, the likelihood is that the elementary predictions of the magnitude of the effects can be sometimes modified by other features of the source mechanism, the geological variations along the wave paths and within the fault zone. Third, the ratio of peak horizontal ground motion in the forward direction of fault rupture to the peak motion in the backwards direction is probably greatest for ground displacements and velocities and least for peak accelerations. High frequency ground accelerations show variations due to scattering, attenuation, and source asperities that mask directivity effects.

The conclusions are based largely on analyses of strong ground motions recorded in the 1979 Coyote Lake, 1979 Imperial Valley, and 1980 Livermore earthquakes, all in California. Each earthquake provides positive evidence for a measurable but variable directivity focusing.

PREFACE

This report was prepared by Dr. Bruce A. Bolt, Seismographic Station, Department of Geology and Geophysics, University of California, Berkeley, under contract DACW39-82-M-1125. It is part of ongoing work at the U. S. Army Engineer Waterways Experiment Station (WES) in the Civil Works Investigation Study, "Methodologies for Selecting Design Earthquakes," sponsored by the Office, Chief of Engineers, U. S. Army. The technical monitor is Mr. Paul R. Fisher of the Office, Chief of Engineers, U. S. Army.

A number of sections summarize and otherwise depend heavily on work of Dr. J. P. Singh. As indicated in the references, the detailed analysis is available in "The Influence of Seismic Source Directivity on Strong Ground Motions," Ph.D. Dissertation, U. C. Berkeley, 1981. Special thanks for discussions and other assistance are made to Dr. R. Uhrhammer, Mr. N. Abrahamson, and Mr. S. Blakeslee. Assistance with tables and figures was provided by Mr. R. McKenzie.

Preparation of this report was under the supervision of Dr. E. L. Krinitzsky, Engineering Geology and Rock Mechanics Division (EGRMD), Geotechnical Laboratory (GL), and the general supervision of Dr. D. C. Banks, Chief, EGRMD, and Dr. W. F. Marcuson III, Chief, GL.

Commander and Director of WES during the preparation of this report was Colonel Tilford C. Creel, CE. Technical Director was Mr. Fred R. Brown.

CONTENTS

PART I

THE PROBLEM

1.1 Objectives of Study

Major modern extensions of the model of elastic rebound along a rupturing fault proposed by H. F. Reid following the 1906 earthquake relate to the progression of the dislocation along the fault. The movement of the source immediately introduces effects on the generated seismic waves because of the relative motion between the dislocation and the surrounding rock. Although actually contained in Reid's discussion, it is only recently that the problem of seismic wave generation by a moving source has been studied quantitatively, either theoretically or from the point of view of the effects on ground motions of interest to engineering and structural design.

The main object of this paper is to describe available evidence for effects of moving sources in earthquakes and to analyze them in terms of the available physics of wave emission. Based on this survey and analysis, some suggestions are made on the significance and incorporation of the effect in strong ground motion estimation. The study is addressed mainly to questions arising in geotechnical studies for engineering purposes. The importance of the moving source effect has been raised but little discussion is available on it in textbooks; it is hoped that this general report may be helpful.

As the theory of the emission of sound from a moving acoustic source indicates,simple directivity factors can be derived in mathematical form which take account of the case in which waves are produced by a finite line source travelling at uniform speed in a fixed plane. Even in this case,

however, the waves produced are not, in general, plane waves and the mathematical analysis is not elementary. In practical problems, where comparisons between theoretical models and actual observed strong ground motions are to be made, additional complications are likely because of variations of speed and intensity (e.g., changes in stress drop) along the dislocation front. In actual earthquakes, the fault zones are seldom simple planes separating perfectly elastic media. Another complication is that, at least in the case of large magnitude earthquakes, the moving source of the earthquake progresses within a definite fracture zone produced by previous faulting. The new dislocation or re-direction in this case occurs in a zone which may resemble a seam of lower velocity and higher attenuating material than the surrounding country rock. In research work that has grown out of this study, source models with such seams are being investigated to determine the effect of these more realistic geological conditions on the generation of the elastic wave field by the moving source.

Finally, it is necessary to define the words "focusing" and "directivity" used in the title of this report. Wave focusing normally means the concentration of wave energy by variations in the refractive indices of the transmitting media, as in focusing of light by an optical lens or focusing of P and S waves by changes in the elastic moduli at structural boundaries. The usage here is different. It is meant to describe an azimuthal change in wave energy around the seismic source due to the moving rupture. This azimuthal dependence is a function of the direction of rupture and hence is described as a directivity effect. In theoretical seismology, the ratio of the spectral displacements of the seismic waves at two diametrically opposite points of the fault plane is termed the directivity (see Part III).

For these reasons, it seems simplest to refer to the radiation effect discussed here as "directivity focusing."

1.2 The Seismic Source Model

The accepted physical source model for tectonic earthquakes is a rupture which extends over a fault plane in the rocks of the Earth (Figure 1.1). The rupture progresses as a series of dislocations after initiating at some point (called "the seismic focus"). A dislocation travels with various rupture speeds which are governed by patches of roughness or asperities along the fault itself. At the dislocation front, the rock slips in a finite time, called "the rise time," and thus produces an elastic rebound of each side of the fault. The elastic rebound reduces the strain and hence the stress along the fault, giving rise to local "stress drops." As the released elastic strain energy is converted to local heat energy and wave energy, the seismic waves are generated near the dislocation front and are radiated away from the moving seismic source.

Small earthquakes can be modeled as essentially point sources because the dislocation front moves only a few kilometers away from the focus. On the other hand, earthquakes with engineering significance involve rupture lengths of tens, and even hundreds, of kilometers in the greatest seismic sources. The appropriate mechanical model must therefore take account of the movement of the source over a finite area with the consequent superposition of radiated waves of various kinds from all parts of the ruptured front. In this model, the duration of strong shaking is dependent upon the dimensions of the faulted surface. The length of time it takes for a train of seismic waves to reach a certain point will depend upon the total duration to complete the dislocation process (involving the rupture velocity) as well as the average seismic moment of the earthquake and the size of the stress drops along the fault.

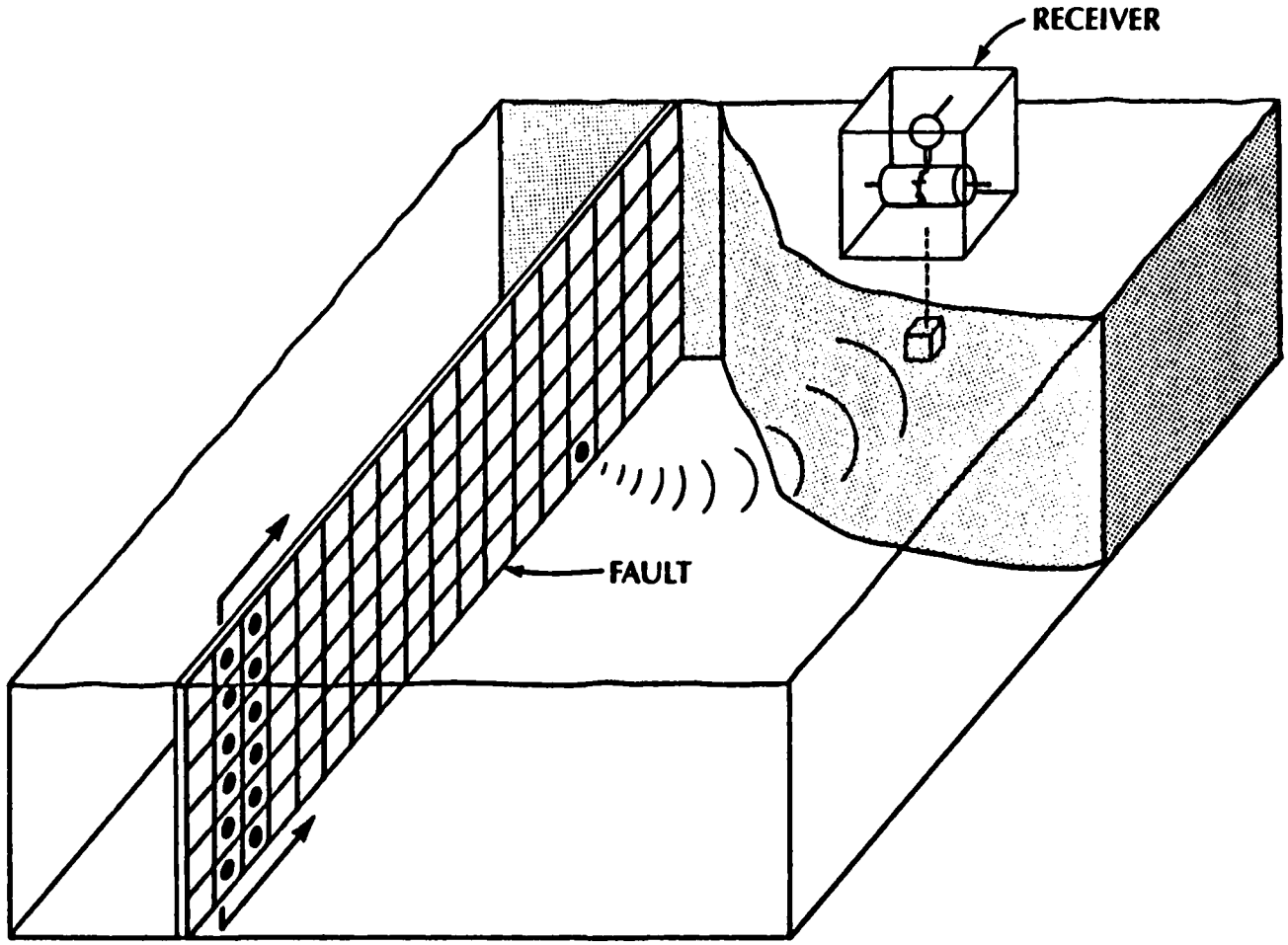

Figure 1.1 A Unidirectionally Propagating Rectangular Strike-Slip Fault Model Represented by Moving Point Sources (After Singh, 1981)

Deviations from the mean duration from earthquake to earthquake are observed and this is often due to the multiplicity of the earthquake source. Many earthquakes are observed to have extended durations which are explicable in terms of the addition of a number of earthquake ruptures in succession along the fault. An important example is the 1940 Imperial Valley earthquake; a comparison of accelerations at the same site between the colocated 1940 and 1979 earthquakes is given in Figure 1.2. An explanation is decrease in the speed of the dislocation (sometimes to zero), followed by a readjustment of the elastic strain and the reinitiation or acceleration of the rupture. The process may be repeated so that the full earthquake is produced by multiple later ruptures from which body waves propagate to the site before the slower surface waves from the previous ruptures have terminated. If the fault surface has a large distribution of roughness, with asperity barriers from place to place along the fault, then considerable variations in source conditions might be expected to arise; the overall effect would be a train of superimposed multiple shocks in rapid succession. This feature of many large earthquakes complicates the recorded strong motions and makes it difficult to isolate the effects, if any, of single aspects of the rupture process such as directivity focusing.

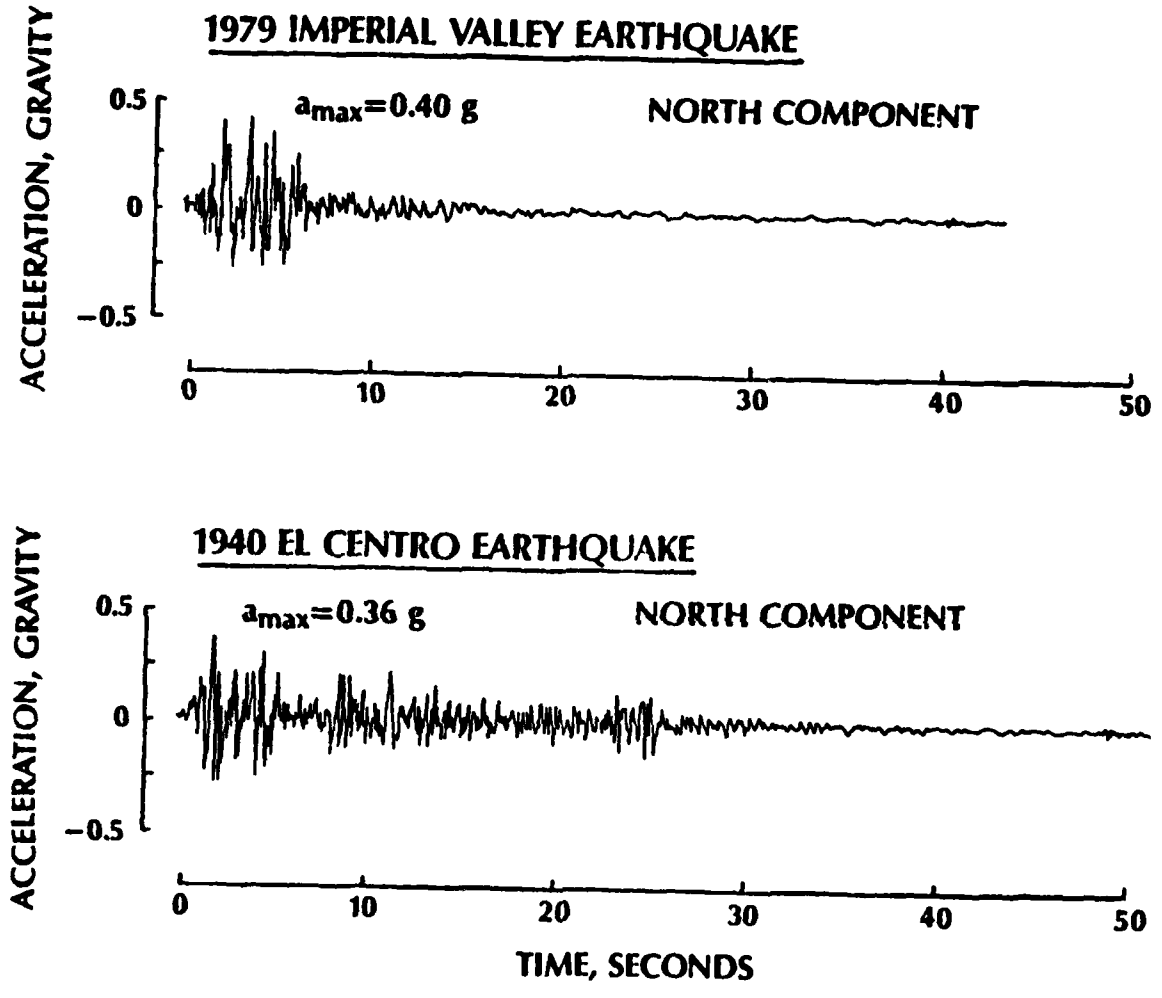

Figure 1.2 A Comparison of Strong Motion Records Obtained at the El Centro Station (North Component) during May 18, 1940, and October 15, 1979, Earthquakes

1.3 Available Evidence

Strong azimuthal patterns in seismic wave radiation have been observed instrumentally in both local earthquakes and teleseisms for many years. From seismic source theory, these radiation patterns have been defined for all types of seismic waves: P and S waves, and Love and Rayleigh waves. These radiation patterns are the basis of the method of fault plane solution using the polarity (or phase) of first motions developed by P. Byerly in the 1930's. The Byerly model, however, considers the earthquake source to be stationary. When the moving dislocation is taken into account, major changes can occur in the radiation patterns for the various seismic waves. A considerable amount of observational evidence consistent with such modifications has now been published, although most evidence pertains to motions recorded a considerable distance from the seismic source, i.e., in the far field.

The first strong evidence for the effect of a moving source in seismology was discussed by H. Benioff (1955) in his explanation of the intensity pattern observed in the 1952 Kern County (California) earthquake. The argument was that a result of the propagation of the dislocation along the fault would be different signals received at opposite ends of the fault, with larger intensities of higher frequency in the direction of propagation and smaller intensities and lower frequencies at the opposite end (see Figure 1.3). Early seismological theoretical developments were made by Ben-Menahem (1961), who developed a function for the directivity based on the known theoretical results for a moving source in acoustics (see Appendix B). Ben-Menahem noted that the spherical shape of the Earth provides a simple way to apply directivity functions to the determination of source parameters such as fault length and average rupture velocity.

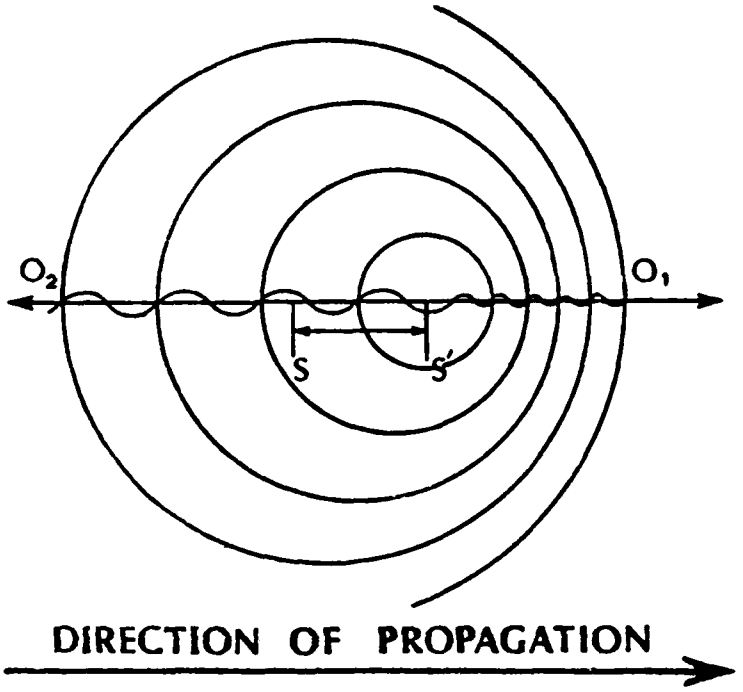

Figure 1.3 Illustration of Sound Waves Proceeding from a Moving Source

Ben-Menahem examined the multiple arrivals of long-period Love and Rayleigh waves, which had circled the Earth a number of times in the case of several major earthquakes. In particular, he showed that directivity effect was present in the great Chilean earthquake of 22 May 1960 and the Alaskan earthquake of 28 March 1964. A recent example of this type of comparison in the far field between theory and observation will be given in Section 4.2.

There is also available more recent seismological evidence, both from the analysis of isoseismal lines relative to the ruptured fault and from analyses of accelerograms recorded near to small and moderate earthquakes in California with well-determined seismic sources (Bakun et al., 1978). It must be stressed, however, that much of the evidence in both categories is of a circumstantial nature; the recordings can be explained in part by directivity focusing, but the explanation is not unique in most cases.

Observed seismic intensity distributions are seldom very precise and are much affected by variations in soil and other surficial conditions. A review of some of the field evidence has been given by J. P. Singh (1981). The theoretical analyses with speculative but plausible models depend significantly on assumptions made concerning both the seismic source mechanism and the crustal structure.

In geotechnical work which endeavors to predict ground motion at a site by the specification of strong ground motion parameters, questions on directivity focusing have been raised seriously only in the last few years. For such purposes, convincing evidence must be available from strong-motion accelerometers in the near field, rather than from sensitive seismographs remote from the source that record small ground motions. At the present, there are only a few such cases (and these from California) where instrumental evidence is available on the question of whether significant directivity effects occur close to the seismic source. The most valuable cases, discussed in Part IV, involve the 1979 Coyote Creek, the 1979 Imperial Valley, and the 1980 Livermore Valley earthquakes.

1.4 Engineering Consequences

The problem of the significance of directivity focusing in the prediction of strong ground motion as a basis for engineering design has arisen already in practice. The thrust of the argument is that, for near fault sites, unless effects of directivity are included in ground motion estimation, the results may under-estimate the actual maximum amplitudes of the ground shaking. An important illustration which will be referred to at several places in this report relates to arguments put before the Nuclear Regulatory Commission that directivity be included in seismic analysis for the Diablo Canyon Nuclear Power Plant site, on the coast of central California. This site is only 4-5 miles from the Hosgri fault on which a Richter magnitude (M_L) 7.5 earthquake was postulated.

It should be emphasized that seismic directivity focusing is of geotechnical interest only as a special near-field earthquake ground motion effect which may be experienced at a site towards which fracture propagation progresses. In theory, the effect of such focusing is to cause local amplification of the ground motion associated with the earthquake. It is suggested that this may be a crucial consideration in structural design because such focusing might significantly increase the spectral components of ground motion employed as input to the seismic design of critical structures. In the case of the site of the Diablo Canyon nuclear plant, it was argued that a major earthquake (M_L = 7.5) associated with rupture along the Hosgri fault zone may produce unexpectedly high accelerations in certain directions.

In its discussion of the question, the Safety and Licensing Appeal Board (Document No. 50-2750L and 50-3230L) even raised quite specific

issues and, for example, stated: "Interveners and the applicant have suggested that the strong-motion data obtained from stations along the direction of the Imperial fault (in the 1979 Imperial Valley earthquake) evidence the 'focusing of earthquake motion.' Yet when the acceleration data of two such stations, El Centro Arrays Nos. 6 and 7, are plotted as a function of distance from the fault, the horizontal acceleration values fall well below the regression mean line for 1 km distance. The vertical acceleration values are also lower than the mean on such a fault. To the extent possible, the parties should analyze the seismic records of this earthquake as they pertain to the focusing phenomena and relate the results of such analyses to the likelihood that focusing might result in amplified seismic motion."

It is now generally accepted, based on the earthquake source models discussed above, that directivity focusing occurs in every earthquake to some degree. It is still a matter of debate, however, whether in most cases the seismic source is organized and coherent enough to affect materially, by means of source directivity, all high-frequency amplitudes (e.g., peak ground accelerations) as a function of azimuth (particularly concentrated in a narrow cone along the ruptured fault).

Further practical aspects of the matter related to assessment of ground motions for engineering purposes and hazard analysis will be discussed in more detail in Section 5.2 after the various lines of evidence are reviewed.

PART II

INTENSITY INFORMATION ON DIRECTIVITY

2.1 Seismic Intensities in Great Earthquakes

According to some theoretical estimates of the effects of directivity focusing, the amplitudes of seismic waves travelling ahead of the moving dislocation might be greater by an order of magnitude than those propagating in the opposite direction of the dislocation. Such theoretical results must be interpreted in terms of the frequencies of the waves and the rupture conditions. Because, for example, all ruptures propagate upwards from the focus, to a certain extent every major earthquake contains the effect of directivity focusing at points on the surface where the rupture breaks out.

Another important aspect is the occurrence of simultaneous dislocation in various directions along the fault surface. It is known, for example, that the fault source in many earthquakes ruptures in a bilateral manner, with the rupture extending away from the focal region in opposite directions. An example of bilateral rupture is the San Andreas dislocation in the 1906 San Francisco earthquake where rupture commenced somewhere off the Golden Gate of San Francisco Bay and propagated both to the north and to the south for hundreds of kilometers. In many other earthquakes, it has been established that rupture is predominantly unidirectional; examples may be found in damaging Turkish earthquakes along the Anatolian fault (Richter, 1938) and in the 1966 Parkfield earthquake.

With these source complexities in mind, intensity studies from great earthquakes provide general information on extent and significance of any amplification due to directivity focusing. In the case of the 1906 San

Francisco earthquake, where detailed field reports are available on damage including many photographs, there is little evidence for enhanced damage due to source directivity. Although the isoseismal map published in the Report of the State Earthquake Investigation Commission shows high intensities along the San Andreas fault break, critical reassessments by G. D. Louderback and others demonstrate that damage to structures was not particularly great along the fault zone in this earthquake (Bolt, 1981). Louderback not only pointed to this fact but also suggested that the reason may well be the presence of gouge and shattered rocks in the fault zone (see Section 3.4).

Another example of a great earthquake which involved surface rupture of a well-marked fault is the 4 February 1976 Guatemala earthquake produced by rupture along the Motagua fault (see Figure 2.1). Espinosa (1976) has drawn attention to the asymmetry in the seismic intensity as shown by the isoseismal lines drawn in Figure 2.1. Rupture progressed from the focus near Los Amates at the east end of the fault to west of Guatemala City. A much larger area of Modified Mercalli (MM) intensities VIII and VI was reported at the western portion of the meizoseismal region and this is consistent in a general way with the concept of directivity focusing. It should be noted that isolated pockets of intensity IX and VIII were mapped at various places along the fault. Field investigations show that at places along the fault rupture damage to certain types of ordinary buildings was not great.

Finally, in any study of seismic intensity, in making any inferences based on field observations, it must be emphasized that damage to structures is likely to arise predominantly from high-frequency motions (in

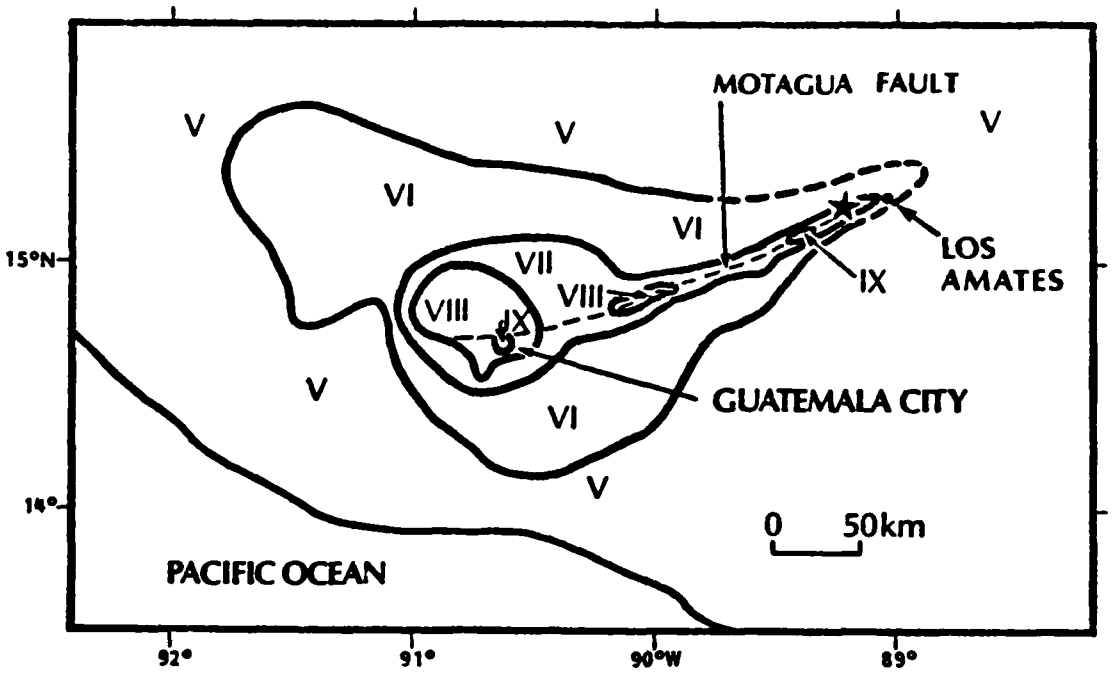

Figure 2.1 Map of Modified Mercalli Intensity Distribution from February 4, 1976 Guatemala Earthquake (from Espinosa, 1976)

the range 2 to 10 Hz). For this reason, observations do not bear directly on the radiation wave pattern due to a moving strike-slip which is observed at very much longer wave lengths at distant seismographic stations.

2.2 Isoseismals in Moderate Earthquakes

Although many isoseismal maps for earthquakes in the United States and elsewhere have been published, few are based on field observations with the precision necessary to make a decisive statement on the effectiveness of directivity focusing. Below a few of the most definitive are mentioned.

One example which led to seismological speculation on the importance of source focusing was the earthquake of 21 July 1952 (M_L = 7.2) in the series of earthquakes in Kern County, California. In this shock, fault rupture began at a focus about 16 km below the surface along the White Wolf fault. It is believed that the rupture extended upward and westward, breaking the surface along the surface trace (see Bolt, 1981). The intensity maps do not plot detailed isoseismals in the meizoseismal area around the fault itself where intensities were VIII or over. Richter (1958) mentions the possible confusion in assignment of intensity arising from the rupture effects at the fault trace itself, a similar circumstance to Louderback's point of the 1906 earthquake. Richter points out, "There was no evidence of extremely violent shaking at points near the trace, as judged by houses. Intensity IX was manifested over much of the area near the fault and effects due to shaking assignable to X were developed in many localities." Another feature of the isoseismal map in this case was the general elongation of the outer isoseismals in the northwest-southeast direction which is parallel to the regional structure, although the White Wolf fault itself trends almost at right angles to this structure.

On the other hand, in this earthquake at the longer periods there was directivity focusing at teleseismic distances. As quoted in Richter's book, "It was found that the amplitude of surface waves for European recordings

were unexpectedly high. However, the amplitudes recorded in Australia and New Zealand were correspondingly low; at those stations the second group of surface waves which had traveled around the world by the major arc was actually larger than the direct waves across the Pacific. These results could be explained in terms of piling of seismic wave energy in the direction in which rupture progressed from the instrumentally determined hypocenter along the White Wolf fault; the speed of progression of such rupture might be expected to be of the same order as that of surface waves. Something related to the Doppler effect would result, with increased concentration of energy in the direction of faulting; this might have contributed to the apparent intensity at Tehachapi." As pointed out at the end of Section 2.1, however, the last comment does not necessarily follow from the directivity evidence at distant stations, because at the teleseismic distances, surface waves have longer periods than the ground motions that damage small structures such as those at Tehachapi.

Other examples of moderate earthquakes in which isoseismals are available are the 1966 Parkfield and the 1971 San Fernando earthquakes (see Bolt, 1981). In these cases, Brune (1978) has stated, "Directivity was probably very important in generating the high velocities observed for the Parkfield and San Fernando earthquakes. ... The concept of focusing or directivity is important in strong motion seismology because, in addition to the effect of radiation patterns, it can introduce large azimuthal variation in ground motion that introduces a large range of scatter in the data, thus making it particularly difficult to estimate the mean and standard deviation of the expected velocities and accelerations from a limited set of data close to the source."

Summary comments on the instrumental evidence in the case of these two earthquakes are given in Section 4.1. As far as the influence of directivity on the isoseismals is concerned, the evidence, however, is not so clearcut. The 1971 San Fernando earthquake had a combined thrust and left-lateral fault source. The intensity distribution for this earthquake is shown in Figure 2.2. The highest intensity area (VII) extends from the fault source towards the southeast in an elongated oval pattern. It is aligned with the direction of slip, rather than parallel to the strike of the fault, in general agreement with the notion that greater energy was propagated in the direction of the moving dislocation.

Two other intensity maps are reproduced here (Figures 2.3, 2.4) for the mainshocks of the sequences near Coyote Lake (6 August 1979) and Livermore (24 January 1980). Although instrumental measurements, discussed in detail in Sections 4.1 and 4.3, indicate significant source focusing effects in the near field of these earthquakes, it will be seen that the isoseismal patterns do not provide much definitive evidence one way or the other. (Information on geological structure and soils would also have to be incorporated in any analysis.) There is, however, a slight indication of extensions of the isoseismals to the southeast of the foci in both cases.

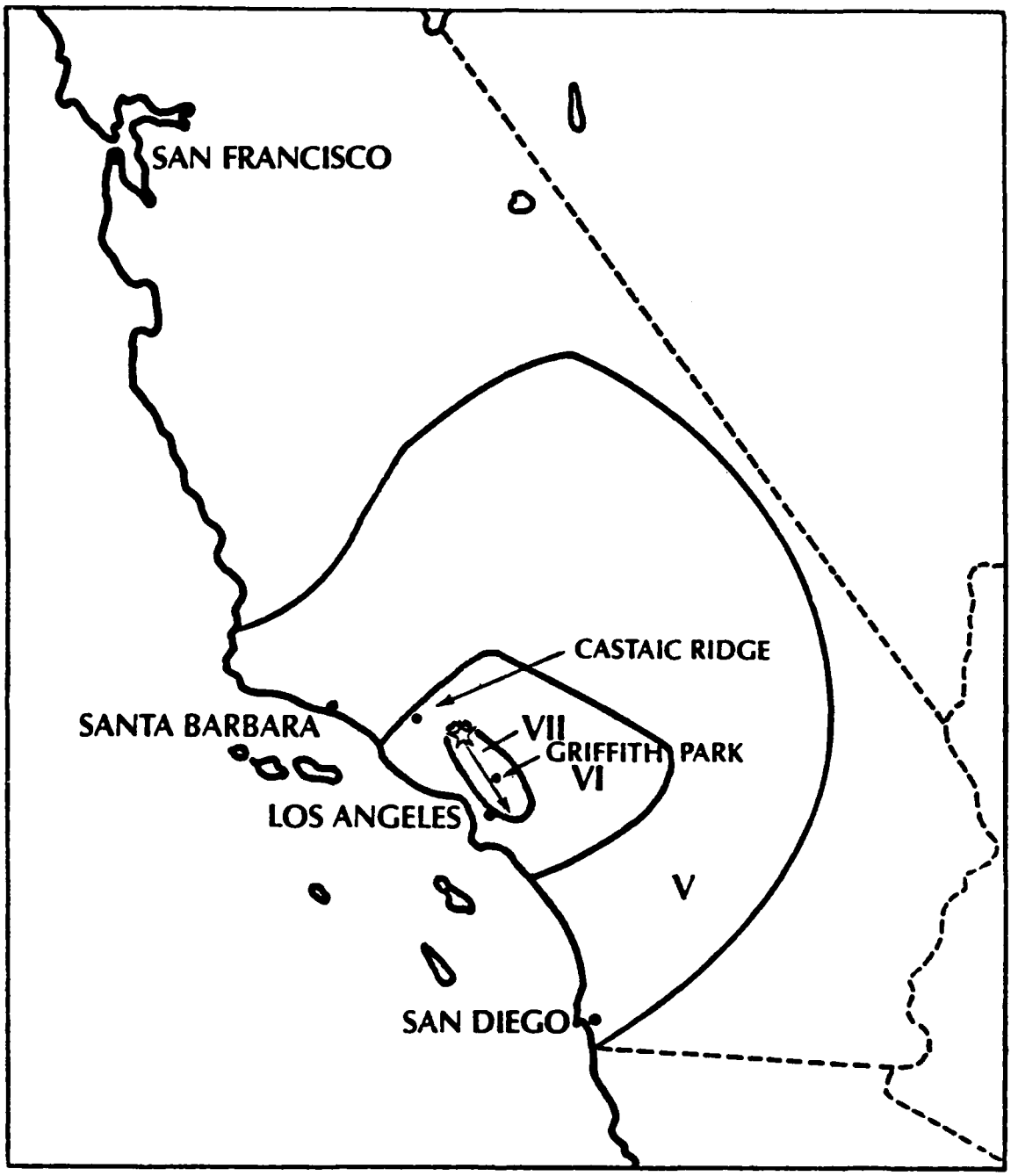

Figure 2.2 Map Showing Modified Mercalli Intensity Distribution of the 9 February 1971 San Fernando, California Earthquake

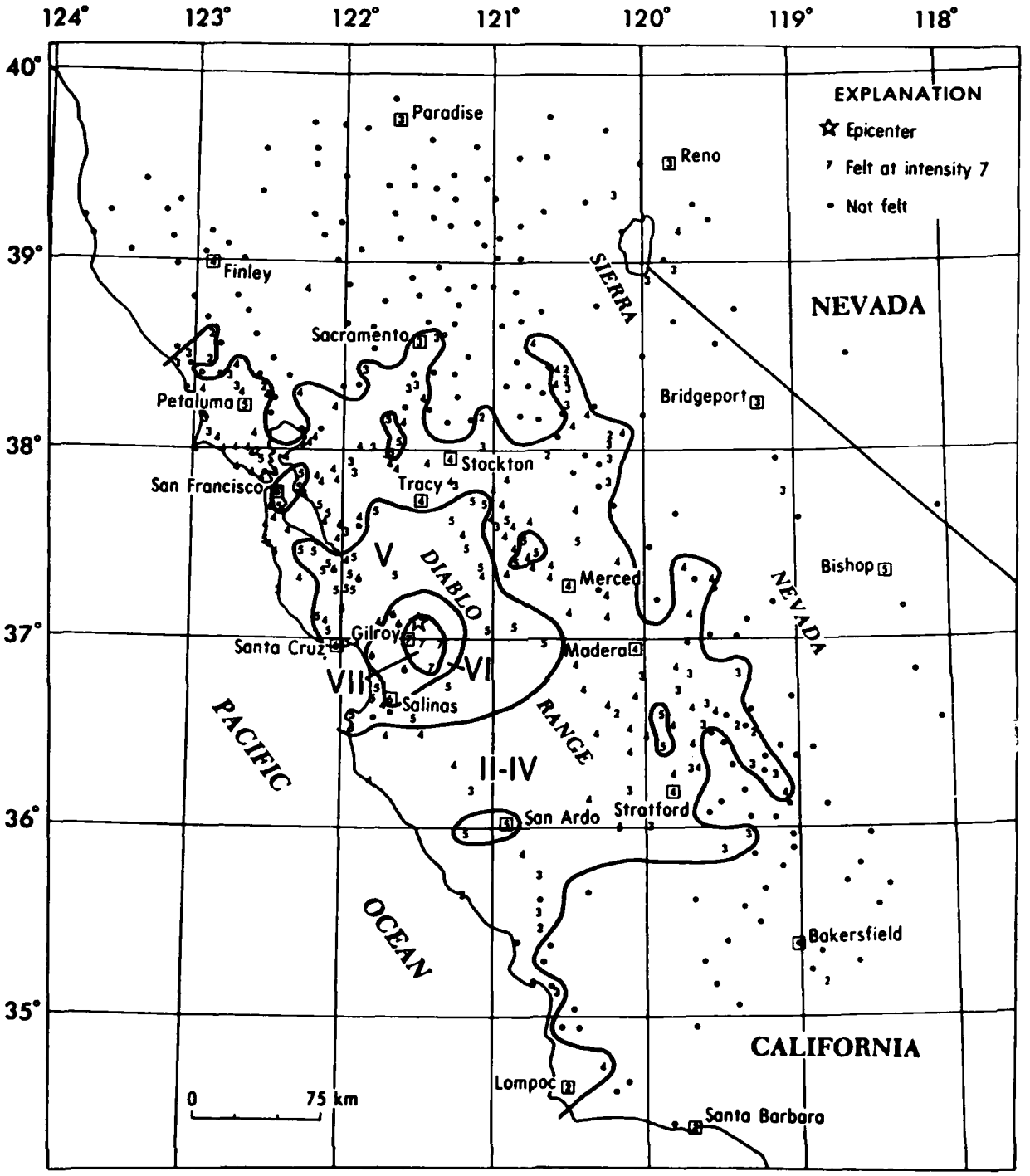

Figure 2.3 Isoseismal map for the central California earthquake of 6 August 1979, 17 05 22.7 UTC. Roman numerals represent Modified Mercalli intensities between isoseismals; Arabic numerals are used to represent these intensities at specific sites.

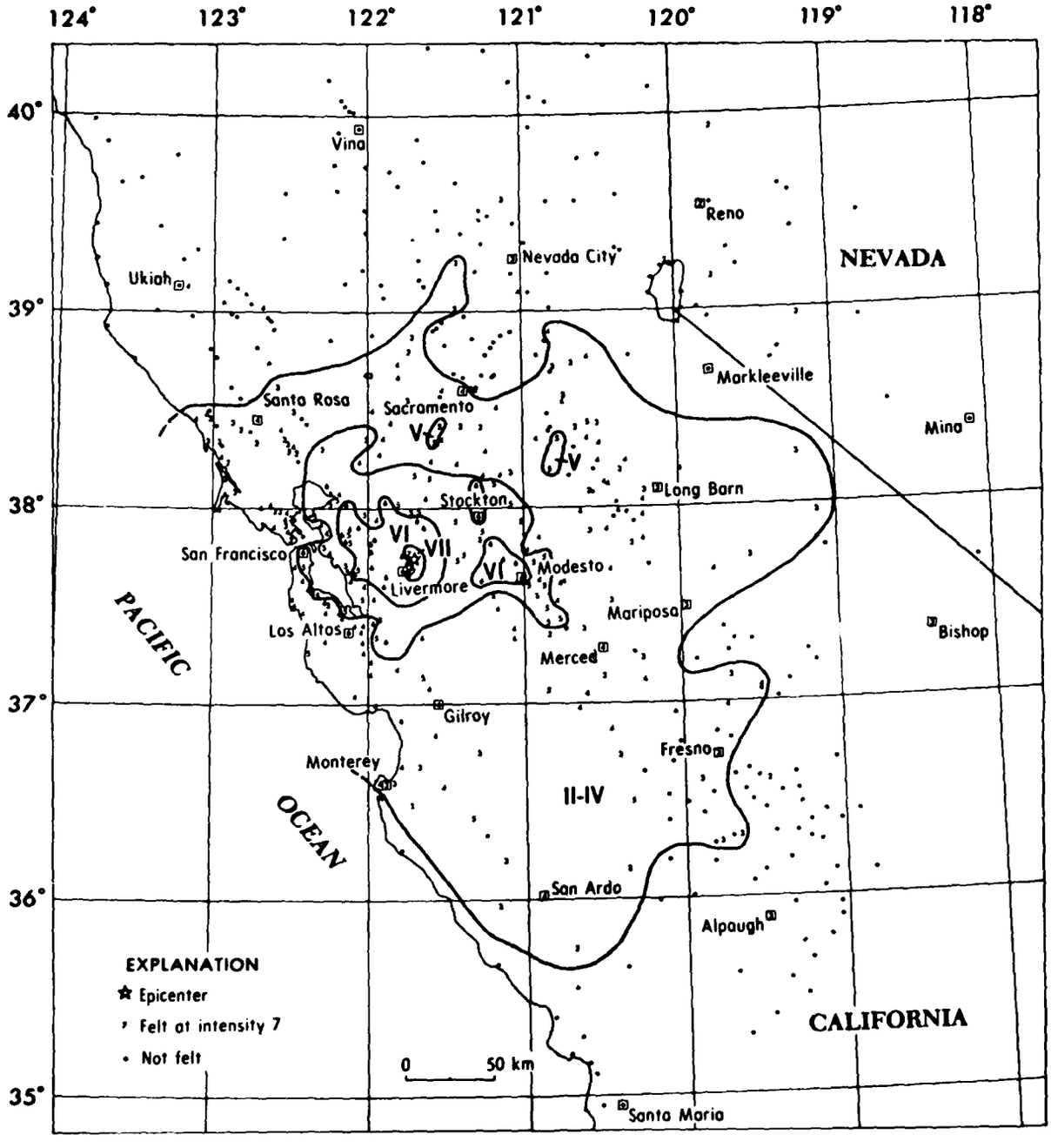

Figure 2.4 Isoseismal map for the central California earthquake of 24 January 1980, 19 00 09.7 UTC. Roman numerals represent Modified Mercalli intensities between isoseismals; Arabic numerals are used to represent these intensities at specific sites.

PART III

THEORETICAL BASIS FOR SOURCE DIRECTIVITY

3.1 Physical Models

The full detail of the patterns of seismic waves cannot be predicted in the near field unless the earthquake source is modeled in a realistic way. The first specification of the physics of the generation of such waves was made by H. F. Reid in his studies of the faulting that occurred along the San Andreas fault in the 1906 San Francisco earthquake. Reid stated that the earthquake vibrations "originate in the surface of fracture; the surface from which they start has at first a very small area, which may quickly become very large, but at a rate not greater than the velocity of compressional elastic waves in the rock." This extract from Reid's description of the elastic rebound theory postulates the propagation of rupture along the fault. Further, Reid stated, "It is probable that the whole movement at any point did not take place at once, but proceeded in regular steps." It is of interest, therefore, that despite this foresight definite consequences of the moving seismic source were not observed instrumentally in earthquakes until seismograms of seismic surface waves at distant stations were compared after the great 1960 earthquake in Chile.

In the mid-1960s, N. Haskell made key contributions to the development of a more physically realistic model and he added details to the way that waves were generated along the fault. He constructed a model "in which the fault displacement is represented by a coherent wave only over segments of the fault and the radiation from adjacent segments is assumed to be statistically independent or incoherent." The physical situation is that the rupture begins suddenly and then spreads with periods of acceleration and

retardation along the relatively weakly welded fault zone. A simplified model of this circumstance is shown in Figure 3.1.

A few years later this Reid-Haskell model was further refined by the introduction of mechanical concepts such as areas of roughness or "asperities" along the fault rupture surface. This representation has been developed by K. Aki and others (see Aki and Richards, 1980) who have further drawn attention to the possible importance of seismic "blocks" or barriers along the fault at which higher strains are required for the moving dislocation to propagate.

It must be emphasized that there is difficulty in making the model of the last paragraph geologically realistic. The estimation of strong ground motion at any point depends not only on the ability to specify a realistic source, but also on the ability to specify a realistic crustal structure in which the rock layers have anelastic and structural properties (including damping) appropriate for the region in question. Most theoretical work to date assumes parallel horizontal layers with soils underlain by rocks of increasing rigidity. Sloping layers with the presence of low-velocity zones and anomalous rock lenses may significantly modify the surface ground motions through well-known wave behavior, such as geometrical focusing, diffraction and scattering of the seismic waves. In the 1979 Imperial Valley earthquake (see Section 4.1), high-frequency waves (particularly on the vertical-component records at many sites) have been interpreted as P waves refracted sharply upwards through surficial sedimentary layers with strong velocity contrasts. These properties of the wave propagation path can be dominant and make the interpretation of a strong-motion accelerogram difficult and non-unique. Unfortunately, detailed crustal structure is not known for most sites, with consequent additional uncer-

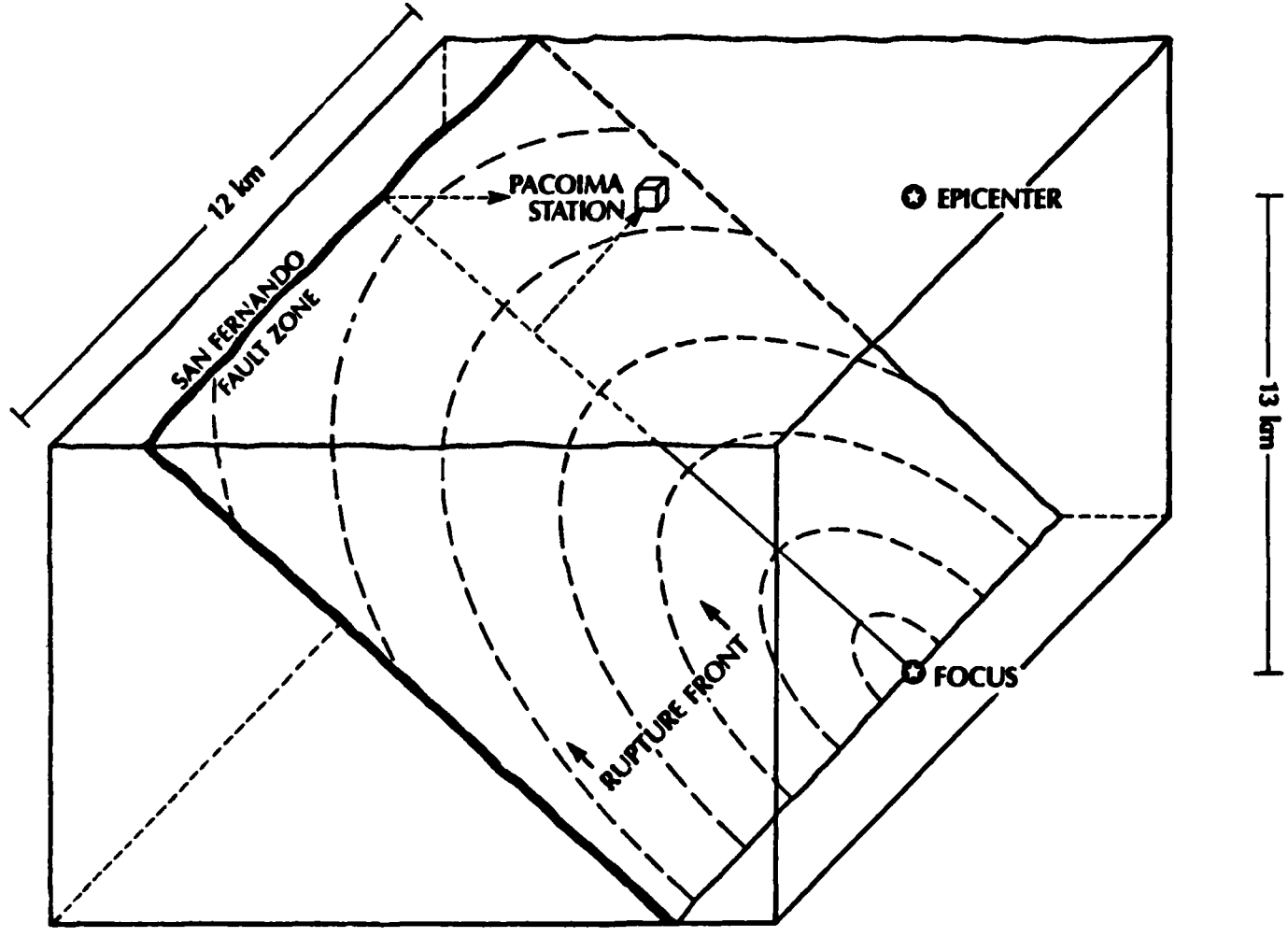

Figure 3.1 Simplified Model of Rupture Surface during February 9, 1971 San Fernando Earthquake in Relation to the San Fernando Surface Faulting, Pacoima Dam, and the Focus (modified from Bolt, 1972).

tainties in the prediction of a strong ground motion.

An Aki-Haskell earthquake source with a high degree of physical realism would be the preferred starting point for the computation of synthetic seismograms of ground motion near to the source so that directivity focusing could be correlated between prediction and observation. A difficulty, in practice, is that, in nearly all cases the detailed asperity and barrier structure along the fault is not known ab initio. Only after the earthquake, can (non-unique) models be contructed to fit the records.

Another critical matter is not emphasized particularly in this report. The physics of earthquake sources indicates that wave patterns generated by moving fault ruptures might be significantly different in certain aspects, depending on the different types of fault rupture involved. Purely strike-slip motion is likely to produce in practice rather different effects on directivity focusing than dip-slip dislocations.

3.2 Kinematics

A stationary seismic fault-slip source can be modeled as a double-couple at a point. It follows that there is already an azimuthal radiation pattern in wave emplitudes even before a rupture velocity is introduced. An example of this azimuthal variation is shown in Figure 3.2. For a simple right-lateral strike-slip fault, for example, the radiation pattern in the near field for S waves will involve four equal lobes with maxima occurring in the direction of the fault and at right angles to it. This azimuthal effect is not related to a source propagation and will always be present for each type of seismic wave considered. Movement of the source produces deformation of the lobes with asymmetrical effects in front of and behind the moving dislocation. Brune (1978) states, "The concept of focusing or directivity is important in strong motion seismology because, in addition to the effect of radiation pattern, it can introduce a large azimuthal variation in ground motion."

For a moving source, waves that leave the traveling rupture in opposite directions will generally have different amplitudes. The kinematic or geometrical effect is simply demonstrated by means of circular wavefronts which are emitted at equal intervals of time from the moving point. The case of a moving point traveling along a straight line is illustrated in Figure 3.3 which was discussed initially in a seismological context by Benioff (1955) in connection with the 1952 Kern Country earthquakes.

The effect of the movement of the source is to change the spectral amplitudes of the waves which leave the source in opposite directions. The ratio of the spectral amplitudes is called the directivity or directivity function (see Appendix B). The formula for the directivity is easily derived from simple kinematic arguments and is given in equation (3.1):

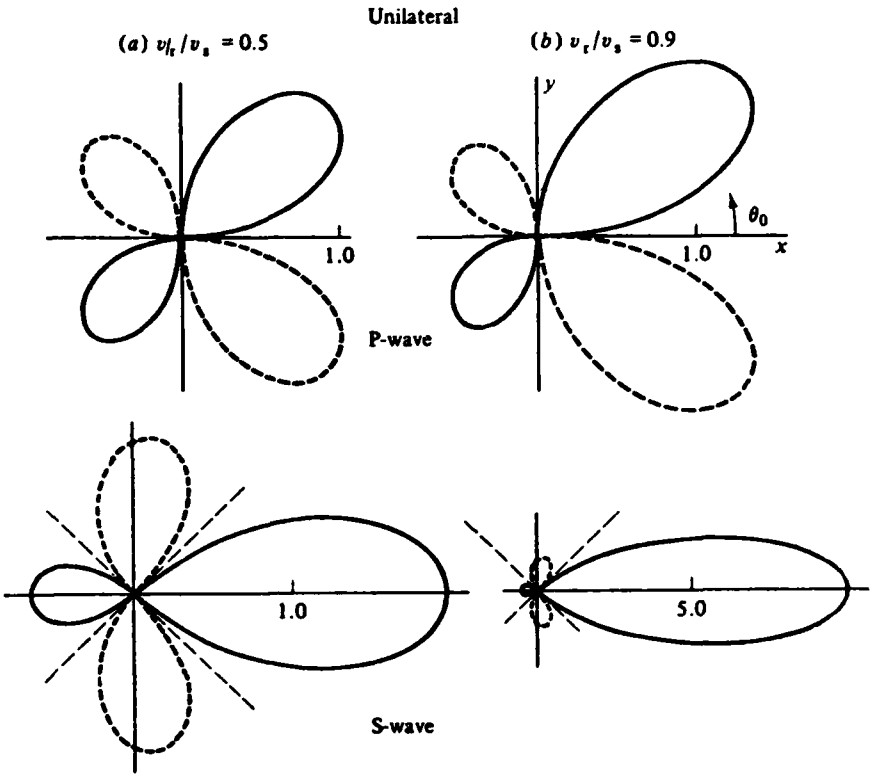

Figure 3.2 Radiation patterns of the P- and S-waves from sources with rupture propagation for: (a) $v_r/v_s = 0.5$; (b) $v_r/v_s = 0.9$, where v_r and v_s denote the rupture and shear wave velocities, respectively. Solid lines indicate positive, and dashed lines negative values. (From Kasahara, 1981)

$$D = \frac{(\frac{c}{v} + \cos\theta_o)\sin\frac{\pi b}{\lambda}(\frac{c}{v} - \cos\theta_o)}{(\frac{c}{v} - \cos\theta_o)\sin\frac{\pi b}{\lambda}(\frac{c}{v} + \cos\theta_o)} , \qquad (3.1)$$

where b is fault length, c is wave velocity, v is rupture velocity and θ_o is azimuthal angle.

The formula assumes that unilateral faulting occurs, that is to say, the fracture along the fault propagates in only one direction. If the fracture moves in both directions, as in bilateral faulting (see Section 3.1), then the directivity function is more complicated.

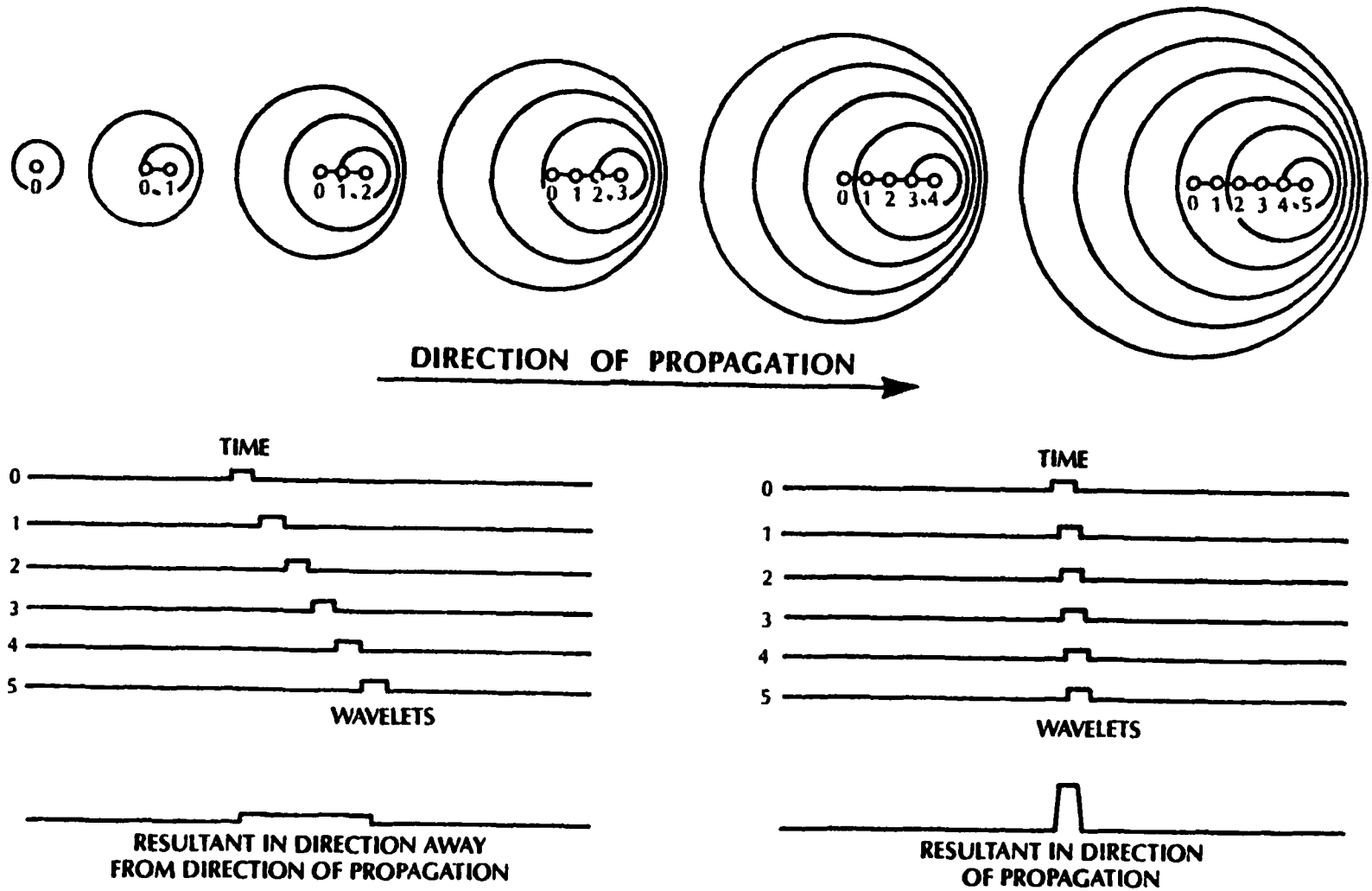

Figure 3.3 Schematic Representation of a Moving Radiating Source and Its Effect on Wave Amplitudes and Shapes (Modified from Benioff, 1955).

For the sake of illustration, consider a vertical strike-slip fault with unilateral fracture propagation. The computed radiation patterns of P and S waves are shown in Figure 3.2. Here the wave amplitudes are plotted in the x-y plane in the case of the unilateral rupture moving in the positive x direction. Rupture velocity ratios are assumed in case (a) $v/c = 0.5$ and in case (b) $v/c = 0.9$ for the shear wave velocity in the medium. (The latter ratio is more realistic.) The effect of the moving source is immediately evident, since for a stationary point source the lobes would show a symmetrical radiation pattern. As discussed in the book by Kasahara (1981), the energy of the seismic wave pulse is approximately constant for different azimuths so that in the positive direction of the x axis where the amplitude becomes very large, the pulse width becomes quite narrow.

It should be emphasized that the discussion given above is a geometrical one and assumes simple geometric configurations. In terms of propagation theory, the waves are assumed to have phase coherence throughout their path, an assumption which may be approximately so if smooth rupture takes place. In many earthquakes, however, as already mentioned, there will be "chattering" of the rupture through patches of roughness on the fault plane and the phase coherence will become very degraded.

3.3 Results from Acoustics

Consider a source of sound moving along a path (Figure 3.4) specified by the position vector $r_s(t)$ with components $x_s(t)$, $y_s(t)$ and $z_s(t)$. The observation point, O, is at a position r with coordinates x, y, z at rest with respect to the medium. The sound pressure observed at r at time t was emitted by the source at time $t_e = t - (R/C)$ at which time the source is at rest $r_s(t_e)$ at the emission point E. The distance $R = r - r_s(t_e)$ between the emission point, E, and the observation point, O, is determined by

$$R^2 = [x-x_s(t-R/C)]^2 + [y-y_s(t-R/C)]^2 + [z-z_s(t-R/C)]^2 \qquad (3.2)$$

More than one value of R satisfies equation (3.2), depending on the Mach number, i.e., the ratio of the speed of source, V, to the speed of sound, C. There are two cases: subsonic or supersonic which are considered separately.

Subsonic case ($M = V/C < 1$)

In the simplest case of subsonic motion the source moves along the x-axis (see Figure 3.4). If the source passes the origin of the coordinate system at time t = 0, then $x_s(t) = Vt$ and $Y_s = Z_s = 0$. Then equation (3.2) simplifies to

$$R^2 = [x-V(t-R/C)]^2 + r^2 = [(x - Vt+MR]^2 + r^2 \qquad (3.3)$$

where $r^2 = y^2 + z^2$.

Equation (3.3) is satisfied by

$$R = \frac{M(x-Vt)\pm\sqrt{(x-Vt)^2+(1-M^2)r^2}}{1-M^2} \quad . \qquad (3.4)$$

For M<1, only the positive sign gives positive R.

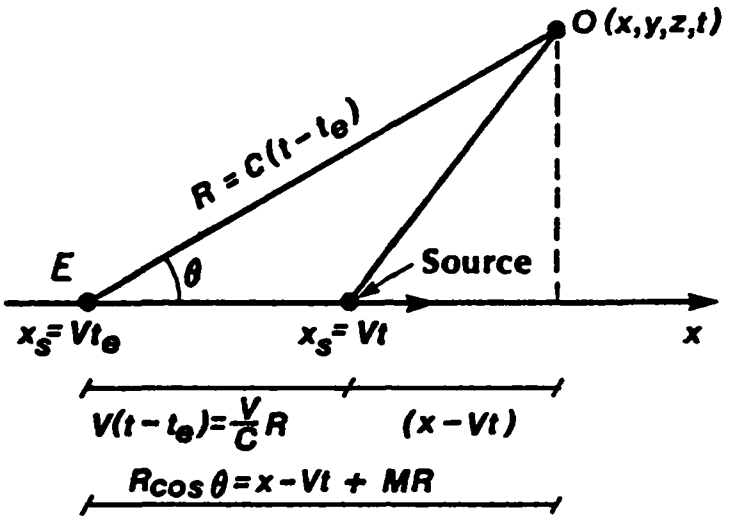

Figure 3.4 Kinematics of a point source in subsonic motion.

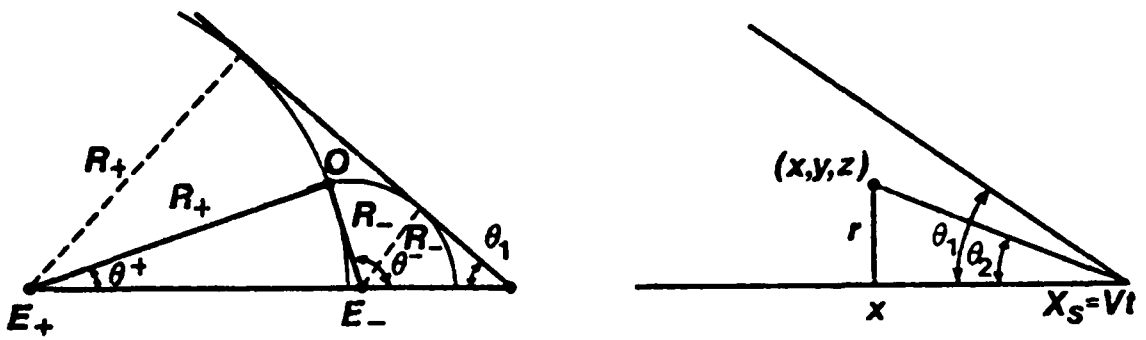

Figure 3.5 Kinematics of the wave field from a point source in supersonic motion.

Supersonic case (M = V/C>1)

For M>1, both plus and minus in equation (3.4) are allowable. Positive R is taken when the point of observation is behind the source, i.e., (x-Vt<C). Then,

$$R_{\pm} = \frac{M(Vt-x) \pm (Vt-x)\sqrt{1-(M^2-1)r^2/(Vt-x)^2}}{M^2-1} \qquad (3.5)$$

Now, let $r/(Vt-x) = \tan \theta_2$ and $\sin \theta_1 = 1/M$ as shown in Figure 3.5, yielding

$$R_{\pm} = \frac{M(Vt-x) \pm (Vt-x)\sqrt{1-(\tan\theta_2/\tan\theta_1)^2}}{M^2-1} \quad . \qquad (3.6)$$

R_+ is real only when $\theta_2<\theta_1$ so that the point of observation is contained inside a cone with the vertex at the source and the vertex angle $2\theta_1$. In this case, two emission points E_+ and E_- can be constructed with emission times corresponding to R_+ and R_- that produce simultaneous contributions to the sound wave field at the point of observation 0 at time t. Thus point 0 lies on the intersection between two phase surfaces (Figure 3.5) which are both tangents to the cone and have their centers (E_+ and E_-) on the x-axis.

For the degenerate case where the observation point, 0, is located along the x-axis, the distinction between the kinematics for subsonic and supersonic sources can be visualized in a simple manner in a space-time diagram (Figure 3.6). In the subsonic case a point, 0, will be reached at a certain time only by the forward-going wave from the source corresponding to the emission point E. In the supersonic case, there is one forward- and one backward-going wave reaching 0 simultaneously, although emitted at different times corresponding to E_+ and E_-.

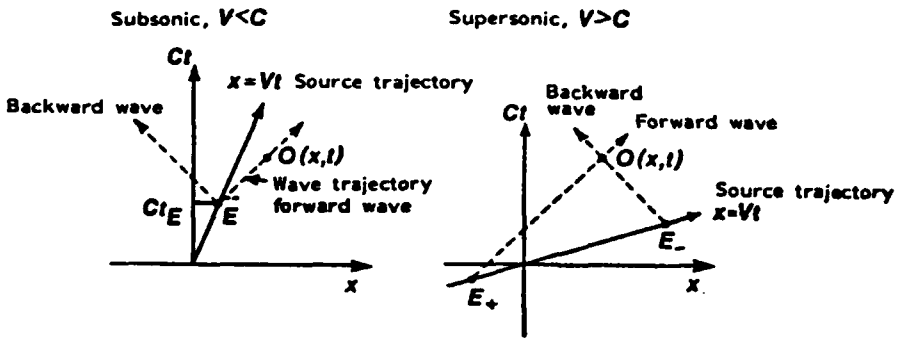

Figure 3.6 Space-time diagrams for the wave kinematics of sources in uniform subsonic and supersonic motions.

The kinematic properties for a moving acoustical source in terms of frequency and amplitude modulation may now be developed. First, consider a monopole source of sound moving with uniform velocity with respect to the surrounding medium. The monopole acoustic source can be thought of in terms of a pulsating sphere, the strength of which is specified by a scalar q.

For the subsonic case, the azimuthal variation of the sound pressure from this moving monopole source can be expressed (Morse and Ingard, 1968) as

$$p = \frac{1}{4\pi R}\frac{q'(t-R/C)}{(1-M\cos\Theta)^2} + \frac{q(\cos\Theta - M)V}{4\pi R^2(1-M\cos\Theta)^2}, \qquad (3.7)$$

where the prime denotes differentiation with time and the first term represents the radiation field with corresponding pressure decrease as R^{-1}. Note that when $\Theta=90°$, the pressure in the far field is the same as when the source is at rest. Quantitative analysis of equation (3.7) shows that the contribution to the total pressure field from the second term in the equation is small (generally, less than about 2-3%). Therefore, dropping the second term, the approximate pressure field is

$$p = \frac{1}{4\pi R} \frac{q'[(t-(R/C)]}{(1-M\cos\Theta)^2} \tag{3.8}$$

This relationship shows that the sound pressure in the direction of motion ($\Theta=0°$) is larger than the pressure in the direction away from the direction of motion ($\Theta=180°$) by a factor $(1+M)^2/(1-M)^2$.

Now let the source strength be harmonic, i.e., $q(t) = q_o \sin \omega_o(t)$. The term q' in equation (3.9) becomes $q_o\omega_o\cos[\omega_o(t-R/C)]$. The pressure field then has the phase

$$\phi = \omega_o (t-R/C)$$

Note that this phase ϕ is not proportional to time alone because R also is time dependent. A generalized concept of frequency can, however, be defined as the time derivative of the phase, i.e.

$$\omega = \frac{d\phi}{dt} = \omega_o \left(1- \frac{1}{C}\frac{dR}{dt}\right)$$

Substitute $\frac{1}{c}\frac{dR}{dt} = \frac{-M\cos\Theta}{1-M\cos\Theta}$ yielding

$$\omega = \omega_o\left(1+ \frac{M\cos\Theta}{1-M\cos\Theta}\right)$$

$$= \frac{\omega_o}{1-M\cos\Theta} \tag{3.9}$$

Equation (3.9) is the Doppler formula for frequency. As the moving source passes the observing point, the angle Θ increases from $\Theta=0$ to $\Theta=\pi$ so that the frequency increases from $\omega_o/(1-M)$ to $\omega_o/(1+M)$.

The Doppler effect is related to the observed intensity distribution of sound. A point in front of the source receives the energy emitted during the time Δt in the time interval Δt_1 which is smaller than the time interval Δt_2 corresponding to a point of observation behind the source.

This result demonstrates that a source which has a symmetric radiation pattern at rest focuses radiation in the direction of motion. If λ_o, ω_o and A_o are the wavelength, frequency and amplitude for the source at rest, then for the case of a moving source the wavelength frequency and amplitude will be modified as shown in Table 3.1 and Figure 3.7.

TABLE 3.1

MODIFICATIONS TO WAVE PROPERTIES

	Forward Direction ($\Theta = 0°$)	Backward Direction ($\Theta = 180°$)
Frequency	$\omega_f = \frac{\omega_o}{1-M}$ (increase)	$\omega_b = \frac{\omega_o}{1+M}$ (decrease)
Amplitude	$A_f = \frac{A_o}{(1-M)^2}$ (increase)	$A_b = \frac{A_o}{(1+M)^2}$ (decrease)
Wavelength	$\lambda_f = \lambda_o (1-M)$ (decrease)	$\lambda_b = \lambda_o (1+M)$ (increase)
Duration	Decrease	Increase

Because for seismic sources such as fault dislocations the observed rupture velocities appear to be less than the shear wave velocity in the strained rocks along the fault, the supersonic rupture case is not pursued further here (but see Section 5.3).

One interesting feature of the supersonic case, however, is the interference among wave contributions from the two emission points E^+ and E^-. These waves with different frequencies and amplitudes give rise to amplitudes of sound pressure that oscillate with time.

Because of the mathematical equivalencies, in appropriate cases, the above theory for a moving acoustical source can be related to P and S waves and surface waves from a moving seismic source. In seismology also, the frequencies and the amplitudes of the seismic wave field will be

modulated by geometrical factors which are a function of a corresponding seismic Mach number M and the azimuthal angle θ between the earthquake source and recording site. The usual factor $x^{-1} \sin x$ in the spectrum of an observed strong motion pulse shape is equivalent in the time domain to a convolution with a rectangular function of temporal duration

$$b\ (1/V - \frac{\cos\ \theta_o}{C})$$

This gives the apparent duration of rupture detected by seismographs along the direction θ_0 for rupture speed V and wave propagation speed C. At higher frequencies, the envelope of $x^{-1} \sin x$ is proportional to ω^{-1}. This smoothing is weakest in the direction of rupture propagation ($\theta_0 = 0$) and strongest in the opposite direction ($\theta_0 = \pi$). As a result, there are more high-frequency waves at $\theta_0 = 0$ than at $\theta_0 = \pi$. This frequency variation is similar to the Doppler effect, which shifts the frequency ω of a moving oscillator by $[1 - V/C\ (\cos\ \theta_0)]^{-1}$. In the case of $x^{-1} \sin x$, the nodes are shifted as a function of θ_0 as

$$\omega_{nodes} = \frac{2n\pi V}{b}\ (1-(V/C)\ \cos\ \theta_o) \qquad n=1,\ 2,\ \ldots$$

The result is destructive interference between waves being generated at different parts of the fault plane; this tends to smooth out high frequencies. In contrast, the Doppler effect does not smooth, because there is only one oscillator.

It should be remarked that in addition to the patterns produced by the factor $x^{-1} \sin x$ there may be other significant factors such as a superposition of sources from multiple complex ruptures and effects from travel path variations. Similar problems of interference also arise for moving acoustical sources. Morse and Ingard (1968) note that near to the

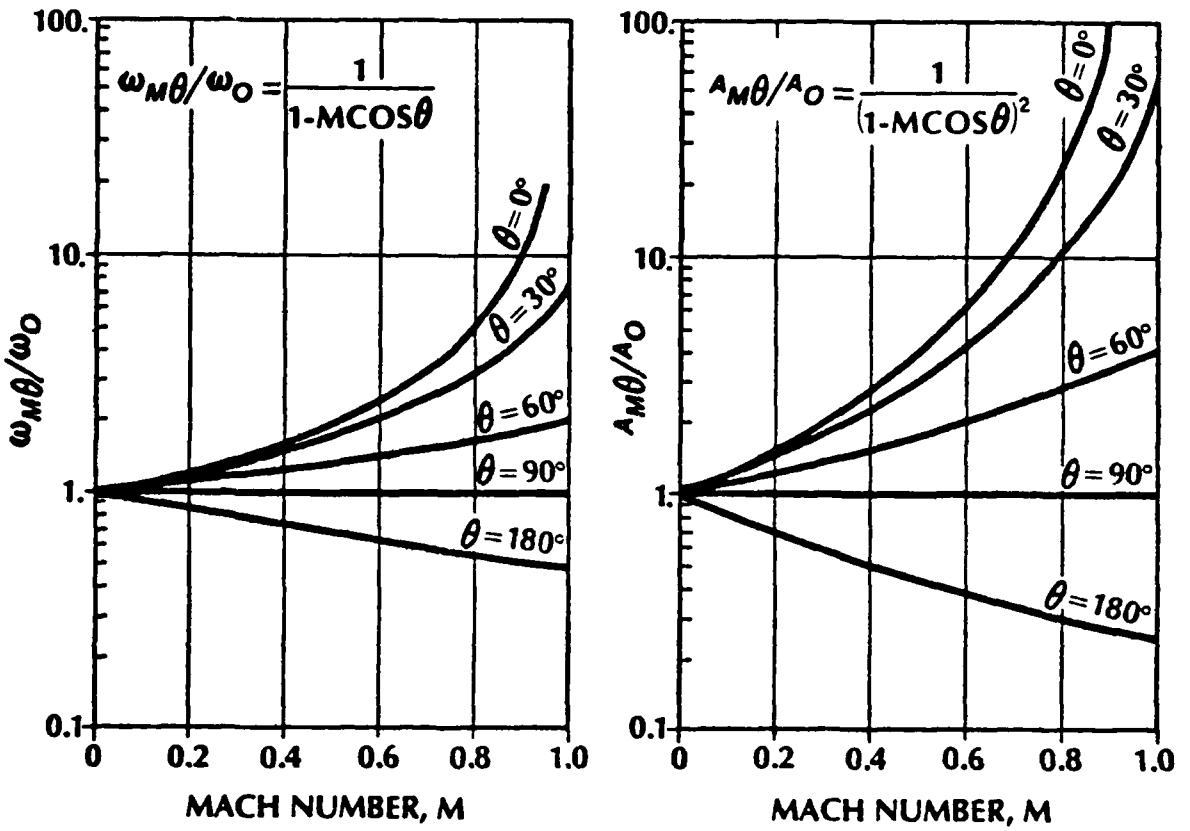

Figure 3.7 The Dependence of Frequency and Amplitude on Mach Number and Azimuth due to a Moving Acoustical Point Source (After J.P. Singh, 1981)

sound source the pressure field is often turbulent and such fluctuations may influence the near field considerably. For example, a design of a train whistle which operated perfectly well in the laboratory ceased to operate at all for train speeds exceeding 50 mph.

3.4 Seismological Results. Seam Waves

As was pointed out in the description of seismic source models given in Section 3.1, most numerical modeling of the earthquake source process has assumed a moving dislocation on a single plane meant to represent the plane of the slipped fault in the crust. Geological conditions, however, along major faults like the San Andreas are significantly different with usually a rather broad zone (up to 500 meters or more in horizontal width) of crushed and sheared rock often containing bands of gouge extending to considerable depth. The question arises as to what extent theoretical predictions for models with a single fault plane separating perfectly elastic media are relevant to the prediction of ground motion in a large earthquake very close to the causative fault zone. Examples of finite zones occur with the San Andreas fault in California and its main subsidiaries such as the Calaveras Hayward fault in northern California and the San Jacinto fault, the White Wolf fault, and the Imperial Valley fault in southern California. To the present, little numerical modeling is available to test the influence of such a zone on the seismic waves generated from a dislocation moving within it.

There would be two effects of the zone. First is the effect to the fault zone structure itself. Geometrically, it resembles a slab or "seam" like a coal seam through country rock. For the sake of clarity in describing this structure, the term "fault seam" will be used herein. The defining properties of the seam would be lower seismic velocity for the rocks within the seam relative to those outside the seam. There would also be a higher attenuation with the seismic parameter Q being up to 20 percent lower on the average than the Q values in the unfractured rock outside the

seam. In practice, of course, gradations must be expected between the properties of the seam and the rock more remote from the major faults in the seam and also variations in properties along the fault zone within the seam. For the purpose of exploration, however, these more complex effects will not be taken into account at the present time.

As the seismic waves are generated by the moving dislocation at depth, it is expected that some of the energy would be channeled within the seam and that these channel waves would be refracted out of the seam; seismic wave energy would leak into the country rock, dependent on the lengths and types of the waves in question. The effect would happen to body waves of both P and S type and to both Rayleigh and Love waves or their equivalents. There would be partitioning in the wave energy between the various types of waves as they interact with the seam boundaries, and special types of trapped waves with appropriate wave lengths might become established (analogous to Stoneley waves which are known to travel under certain circumstances along boundaries between rocks of different properties at depth in the Earth.) Of special importance would be enhanced attenuation of waves which were trapped within the seam; wave energy diffracted out of the seam channel would attenuate less from damping than wave energy within the attenuating seam itself. This effect might be expected particularly to decrease the high-frequency accelerations associated with velocities and displacement (see Singh, 1981).

Theoretical work supporting these ideas may be found in the physics literature, particularly that dealing with the channeling of light, acoustic energy, and elastic waves along ridges and ducts (Morse and Ingard, 1968). As a simple model, there is some resemblance to the well-known

effect of an aperture on a light beam in which diffraction patterns are set up (see Appendix A, Figure A.1). Singh (1981) has drawn attention to the correspondence between the amplitude pattern on the far side of a light aperture and that which he observed in the variation of the peak ground acceleration on the array across the Imperial fault in the 1979 earthquake (see Figure 4.7).

Some numerical analogies come from the study of wave propagation along irregular coal seams (Krey, 1963; Drake and Asten, 1982). It is known that channel or seam waves (see Appendix A, Figure A.1) propagate in the two-dimensional wave guide which is constituted by a seam of low-velocity coal between higher velocity rock layers. These seam waves are both longitudinal (i.e., sound) waves and shear waves which can be studied by seismological methods. Theory indicates that a low-velocity layer supports two classes of seam waves, generalized Rayleigh waves and generalized Love waves. In the latter, the motion is horizontal shear, transverse to the direction of propagation along the seam. Each class of seam waves includes multiple modes which are dispersive.

Recent detailed finite element modeling of waves channeling along coal seams have been carried out by Drake and Asten. They show that waves essentially of Stoneley type can channel along coal seams in both pseudo-Rayleigh and pseudo-Love types but that the efficiency of the channel effect is dependent significantly on the wave mode and on the frequency of the wave. Typical P velocities in the country rock in this modeling were taken as 4 km/sec and 2.1 km/sec, respectively, while within the seam the P and S velocities were 2.4 and 1.28 km/sec, respectively. Although these

models do not include any damping terms in the finite element computation, they do show that the presence of a fault zone with significantly different seismic parameters could have significant consequences as far as directivity focusing properties are concerned.

Another relevant study involves the propagation of elastic surface waves guided by ridges on the surface of an elastic body. The wave guiding action of the linear topographic feature is relevant to the present problem in which we consider the fault zone or fault seam as the wave guide analogy of the raised ridge. Some useful results (Burridge and Sabina, 1972) for such models using finite element methods show that with certain geometric dimensions and elastic constants, guided waves do propagate along the ridge as dispersed trains. The calculations indicate, however, that in any case only some modes may be properly trapped by the linear feature and that this occurs in only certain limited frequency ranges. Again, the calculations indicate that only some modes of wave propagation of pseudo-Rayleigh type propagate in an unattenuated form. In other words, energy is continually leaked from the wave guide into the surrounding material in most cases. By analogy, for the fault seam the amplitude of the waves propagating along the seam would continually fall. As with the coal seam analysis, this interesting modeling work was carried out without any frictional attenuation included in the calculations, so the results can be taken only as suggestive. It is likely, however, that the inclusion of damping would leave the main results unaffected but reduce even more the amount of high-frequency seismic energy able to be propagated to any distance along the seam.

PART IV

OBSERVATIONAL EVIDENCE FROM RECORDED STRONG MOTIONS

4.1 Recent California Earthquakes

In the last few years instrumental evidence of importance has come from a number of moderate California earthquakes. These are the 1966 Parkfield earthquake, the 1971 San Fernando earthquake, the 1979 Coyote Lake earthquake, the 1979 Imperial Valley earthquake, and the 1980 Livermore earthquake. In each case, strong-motion accelerometers recorded the strong shaking in the near field and so some quantitative evidence is available which bears on the question of the radiation wave field from a moving dislocation (see for fuller descriptions, Bolt, 1981). As is usually the case, however, in strong-motion seismology the geographical distribution of strong-motion instrument sites was by no means optimum for the assessment of the quantitative effects of directivity focusing. While the results are helpful, in no case is there a final conclusion to the problem.

The Parkfield earthquake occurred on 28 June 1966 and had M_L = 5.5 and a seismic moment of 1.9×10^{25} dyne-cm. The mean stress drop in this earthquake has been estimated at quite low values of the order of 5 bars. Rupture occurred along a central segment of the San Andreas fault showing predominant strike-slip motion with a maximum slip of about 20-25 cm. The rupture was right-lateral and there is evidence of a mean rupture velocity of between 2.5 and 2.9 km/sec. A small array of strong-motion instruments at right angles at the southern end of the fault rupture recorded the motion and has given information on the attenuation of strong shaking away from the causative fault. However, no strong-motion instrument was available at the northern end of the faulting so a direct calculation of the directivity is not possible.

It is of interest, however, that the strike of the fault is such that its northward projection passes close to the Berkeley stations in the San Francisco Bay area. A study of the spectrum of the recorded waves on a broadband seismograph at Berkeley (Filson and McEvilly, 1973) has given an excellent example of an observed directivity spectral function which fits well the form of the theoretical spectrum for a moving source. This spectrum yields an estimate of the velocity of rupture of about 2.2 km/sec towards the south.

The San Fernando earthquake occurred on 9 February 1971 and had a magnitude of $M_L = 6.5$ and a moment of $M_o = 1.5 \times 10^{26}$ dyne-cm. Various stress drops were originally calculated for this earthquake with an average value of 50 bars. In a careful reassessment, however, Hanks and McGuire (1981) inferred that the major part of the seismic energy was released over a small portion of the fault plane and that the stress drop involved was of the order of 1000 bars.

Surface faulting occurred in the San Fernando Valley and along the foothills of the San Gabriel Mountains in this earthquake. It indicated both thrusting and left-lateral motion. One explanation given for large accelerations recorded at Pacoima Dam (up dip along the thrust fault) is directivity focusing (Heaton and Helmberger, 1979; McGuire and Hanks, 1980). A number of plausible but competing models have been computed for this earthquake source, however, so that available data do not provide the resolution needed for a well-constrained solution.

The Coyote Lake earthquake occurred on 6 August 1979. It had $M_L = 5.9$ and a seismic moment of 6×10^{24} dyne-cm. Minor breaks and cracks occurred along the Calaveras fault for about 8 to 10 km, with right-lateral displacement of up to about 5 mm. It is of special value for studies of

directivity focusing because 24 strong-motion accelerometers were triggered located within 50 km of the fault rupture with several very near to the Calaveras fault. The geometry of the faulting and the location of aftershocks and accelerometers are shown in Figures 4.1 and 4.2. Of particular interest is a comparison (Figure 4.3) of recorded ground motion between the Coyote Creek station to the north and Station 6 to the south, both adjacent to the fault. Comparisons of peak acceleration (PGA), peak velocity (PGV), and peak displacement (PGD) in these records have been made in detail by J.P. Singh (1981). He found that enhanced acceleration, velocity, and displacement recorded at Station 6 compared with the Coyote Creek station are in agreement with directivity focusing. The enhancement is greatest for PGD and least for PGA in this comparison, with the amplification factor reaching 1.8 for PGA, 2.0 for PGV, and 4.0 for PGD. Moreover, higher frequencies were richer at Coyote Creek than at Station 6 (Figure 4.4), perhaps indicating damping in the fault zone.

The Imperial Valley earthquake occurred on 15 October 1979. It had a magnitude of $M_L = 6.6$, and a seismic moment of 8.7×10^{25} dyne-cm. As in the Parkfield earthquake, the estimated mean stress drop in this earthquake is low at about 5.5 bars. Rupture was observed (see Figure 4.5) along the 35 km of the Imperial and Brawley faults and the motion was right-lateral strike-slip (up to 55 cm) with some dip-slip offsets (up to 19 cm) down to the east. Many strong-motion accelerometers, including a 13-element linear array, recorded this earthquake in the near field and provided much hard data on the surface radiation pattern. As mentioned in Section 3.2, theoretical modeling of wave focusing due to moving sources suggests that the zone of wave enhancement is concentrated into a narrow lobe in the direction of the moving fault dislocation (see Figure 3.2).

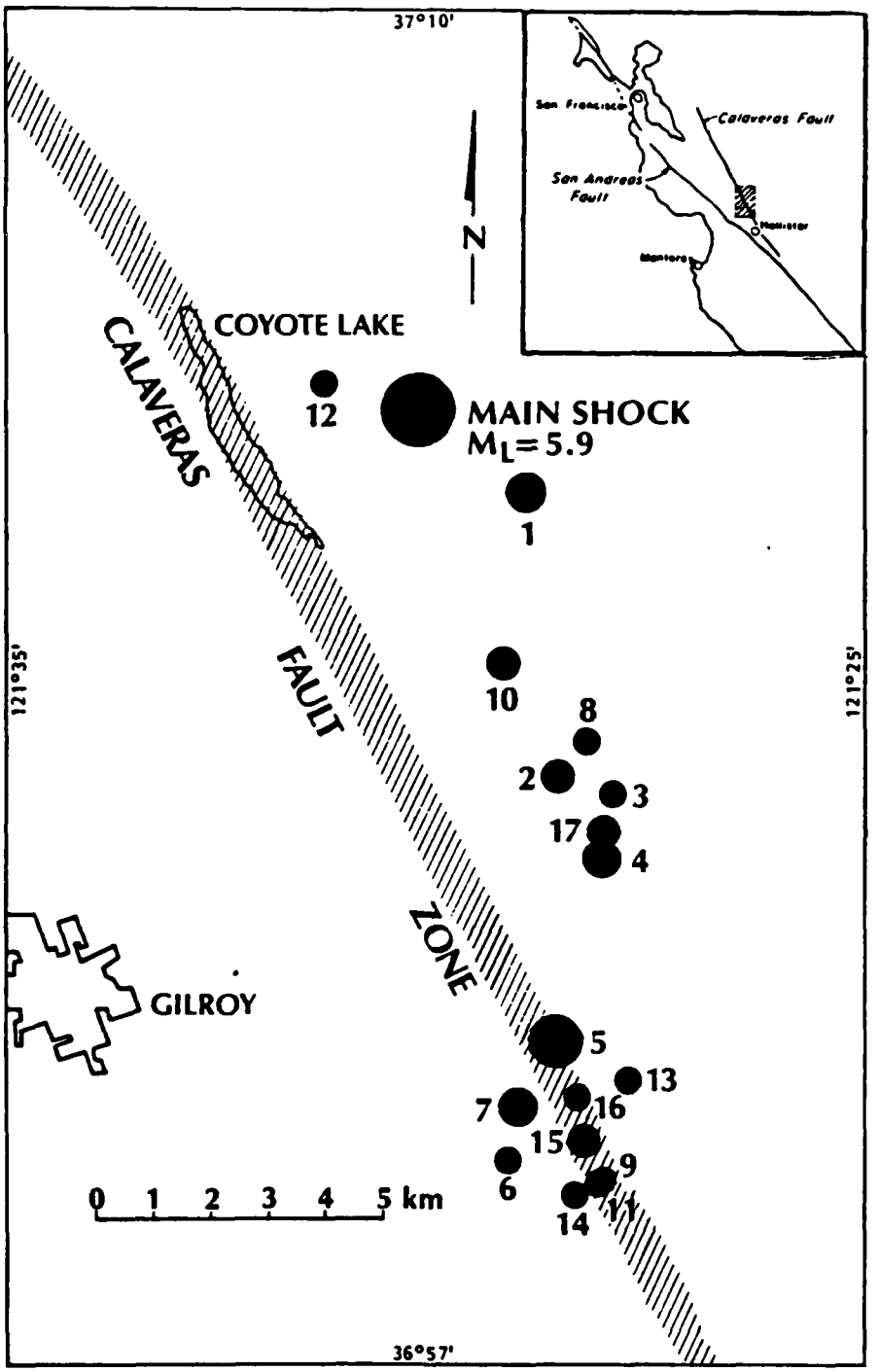

1. Numbered circles correspond to Table 5-1 and their diameter scales to the local magnitude (M_L).
2. Inset shows the relative position of the Coyote Lake area within the central coast region of California.

Figure 4.1 Coyote Lake Earthquake Sequence (Modified from Uhrhammer, 1980)

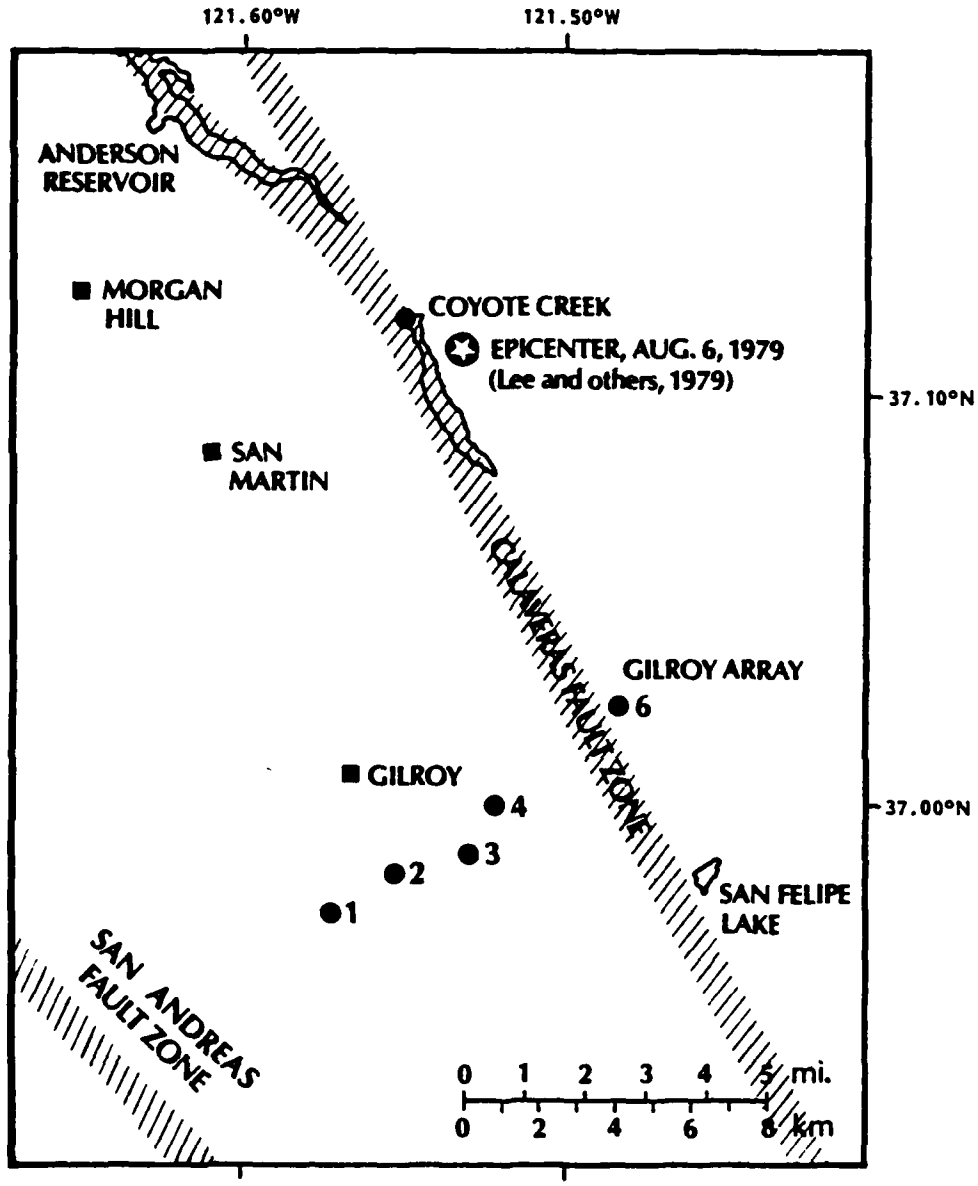

Figure 4.2 Location of Strong Motion Instruments

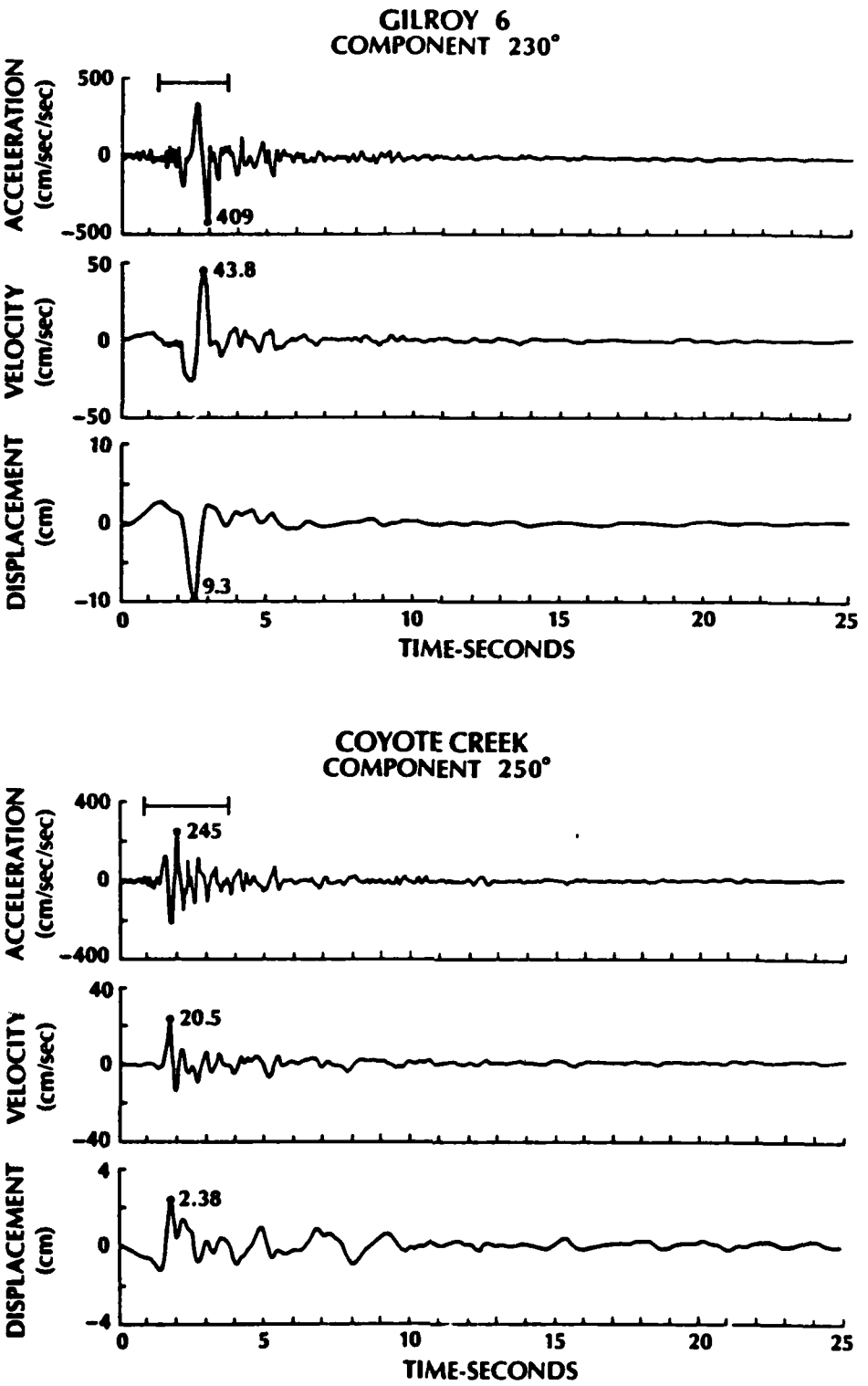

Figure 4.3 Corrected Acceleration, Velocity, and Displacement Records for Stations Coyote Creek and Gilroy 6

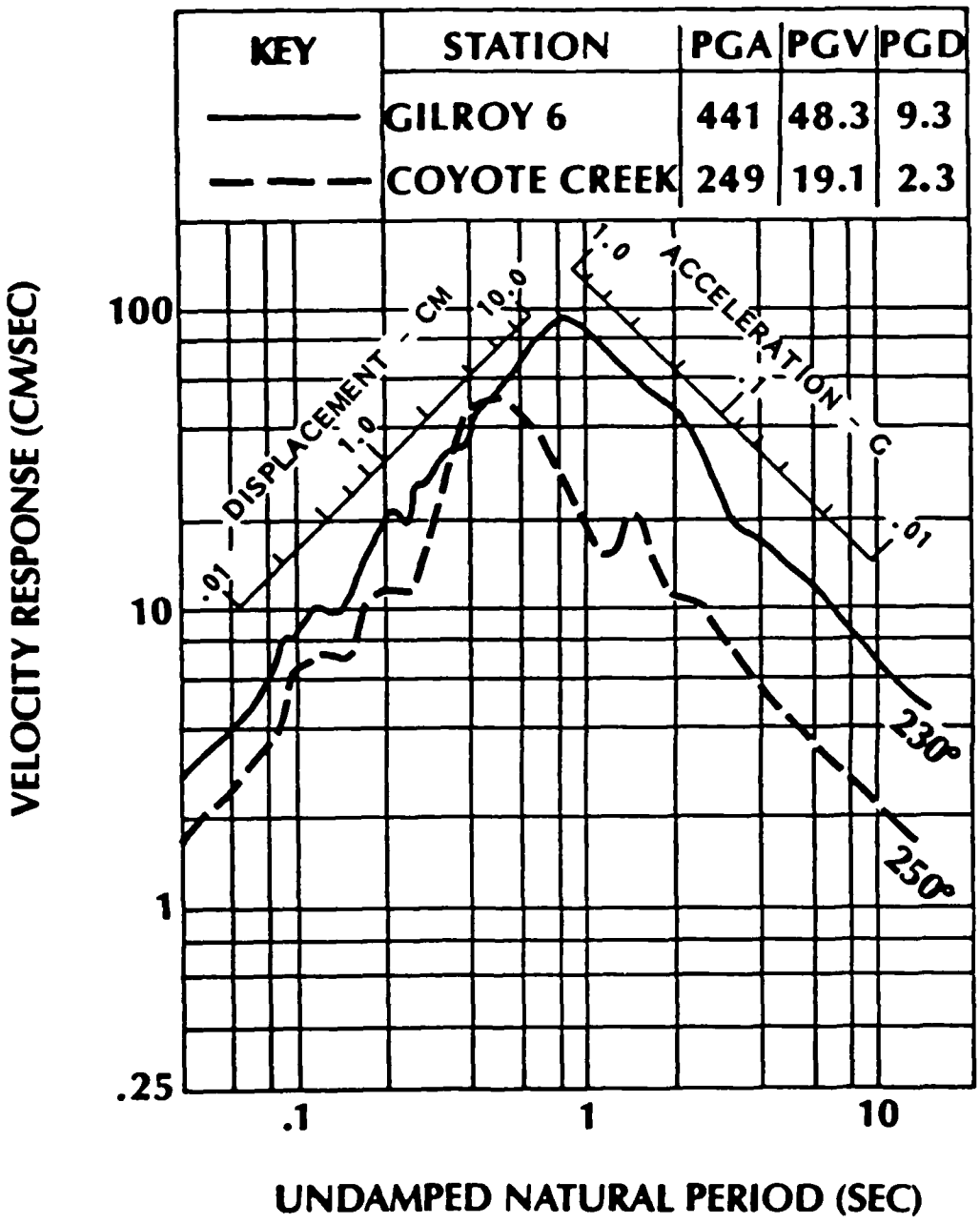

Figure 4.4 Comparison of Response Spectra for Stations Gilroy 6 (230° Component) and Coyote Creek (250° Component) for 5% Damping

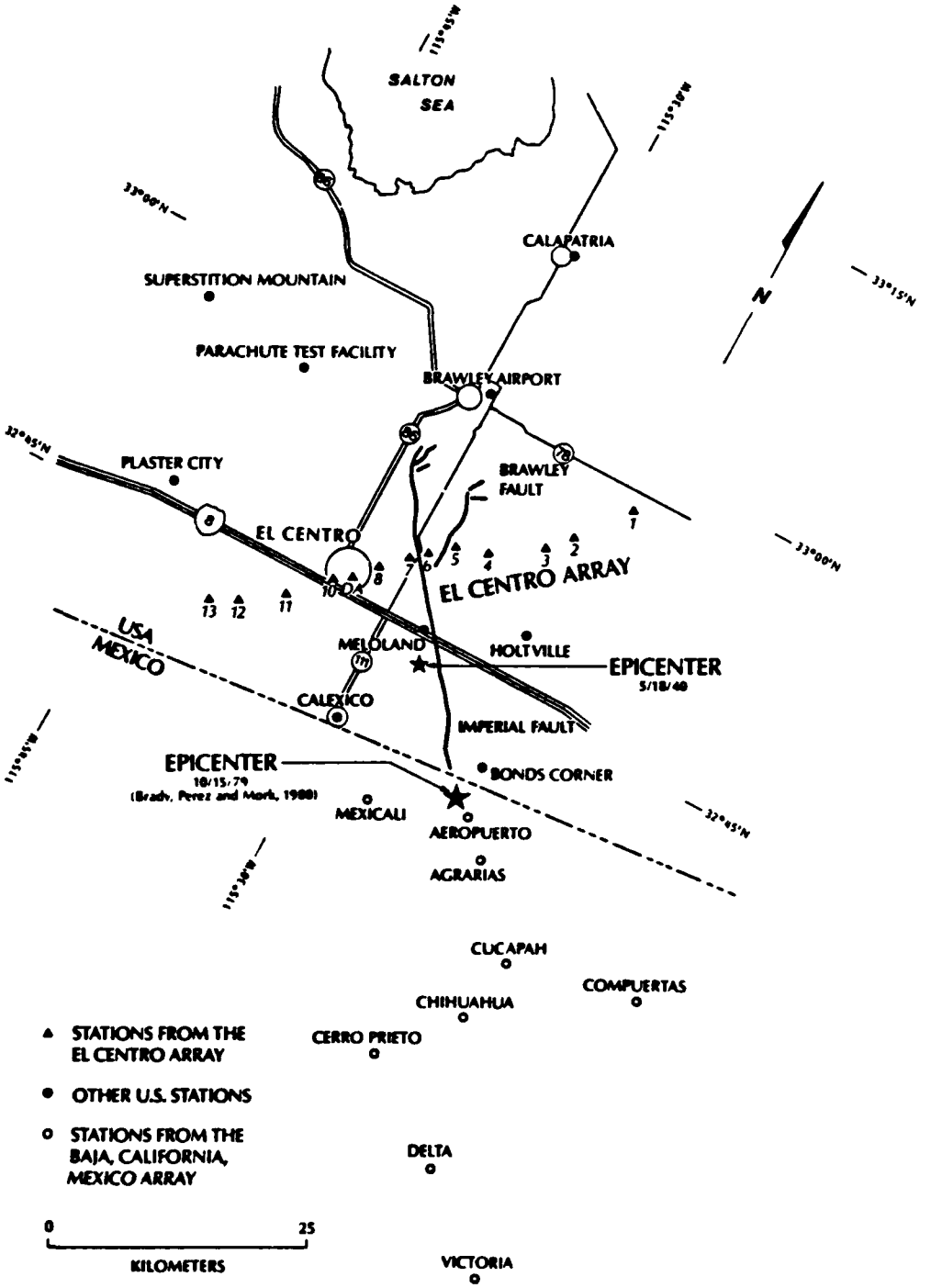

Figure 4.5 Location Map of Strong Motion Instruments (modified from Brady et al., 1980)

Simple models (Brune, 1978) suggest that a focusing lobe has a width of ±5% or so from the direction of the dislocation. In such a circumstance, the restricted lobe of enhanced directivity focusing could be missed observationally unless there are a large number of strong-motion instruments in the near field. In the case of the 1979 Imperial Valley earthquake, with rupture traveling from near the Mexican border northwest beyond El Centro, the accelerograms from Bonds Corner and Station 7 (see Figure 4.6) are within this lobe so that they provide a test of the predictions. The 13-element array, total length 45 km, passing through El Centro provides further discriminatory near-field evidence.

The 1979 Imperial Valley measurements have been extensively analyzed by J.P. Singh (1981) and only the main relevant conclusions are summarized here. At Bonds Corner the recorded PGA, PGV, and PGD (230° horizontal component) were 770 cm/sec^2, 44 cm/sec, and 15 cm, respectively. At Station 6 to the northwest, the corresponding values were 428 cm/sec^2, 108 cm/sec, and 55 cm. The latter values are closely confirmed by readings of 454 cm/sec^2, 108 cm/sec and 41 cm at Station 7. In addition, the bracketed duration at Bonds Corner (230° component) was 13 sec compared with 8 sec at Station 6. This comparison indicates larger peak amplitudes in velocity and displacement ground motions to the northwest (a factor of about 3) consistent with the directivity model but a decrease in PGA in the direction of the rupture propagation.

Another germane comparison is a plot of PGA, PGV and PGD values from the El Centro array (230° component) against perpendicular distance from the Imperial fault (Figure 4.7). The PGV and PGD curves show a roughly unimodal curve with maximum values extending 1-2 km to the west of the fault and 5-6 km to the east. Outside this central maximum, wave attenuation

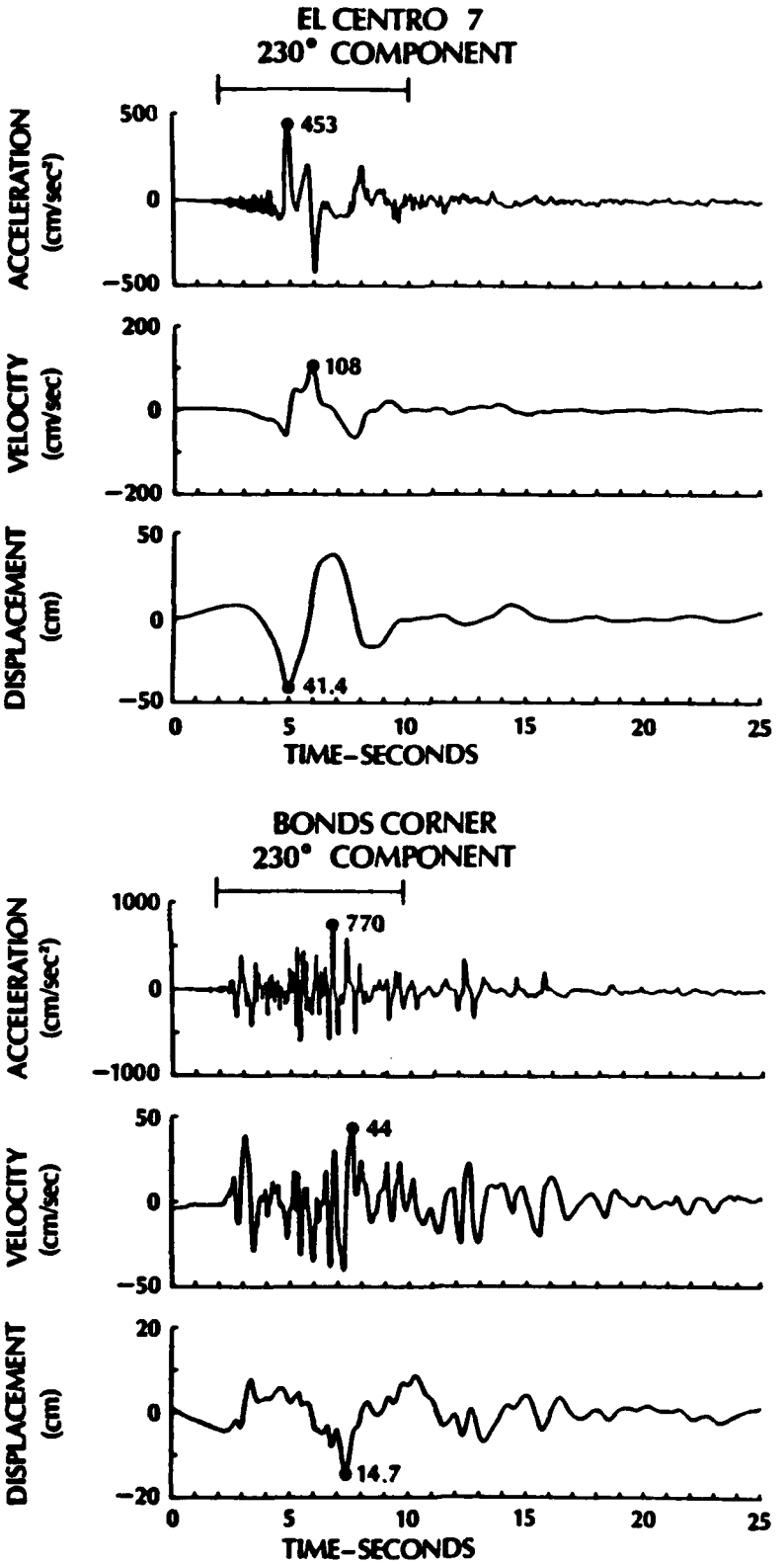

Figure 4.6 Corrected Acceleration, Velocity, and Displacement Records for Stations, Bonds Corner, and El Centro (230° Component)

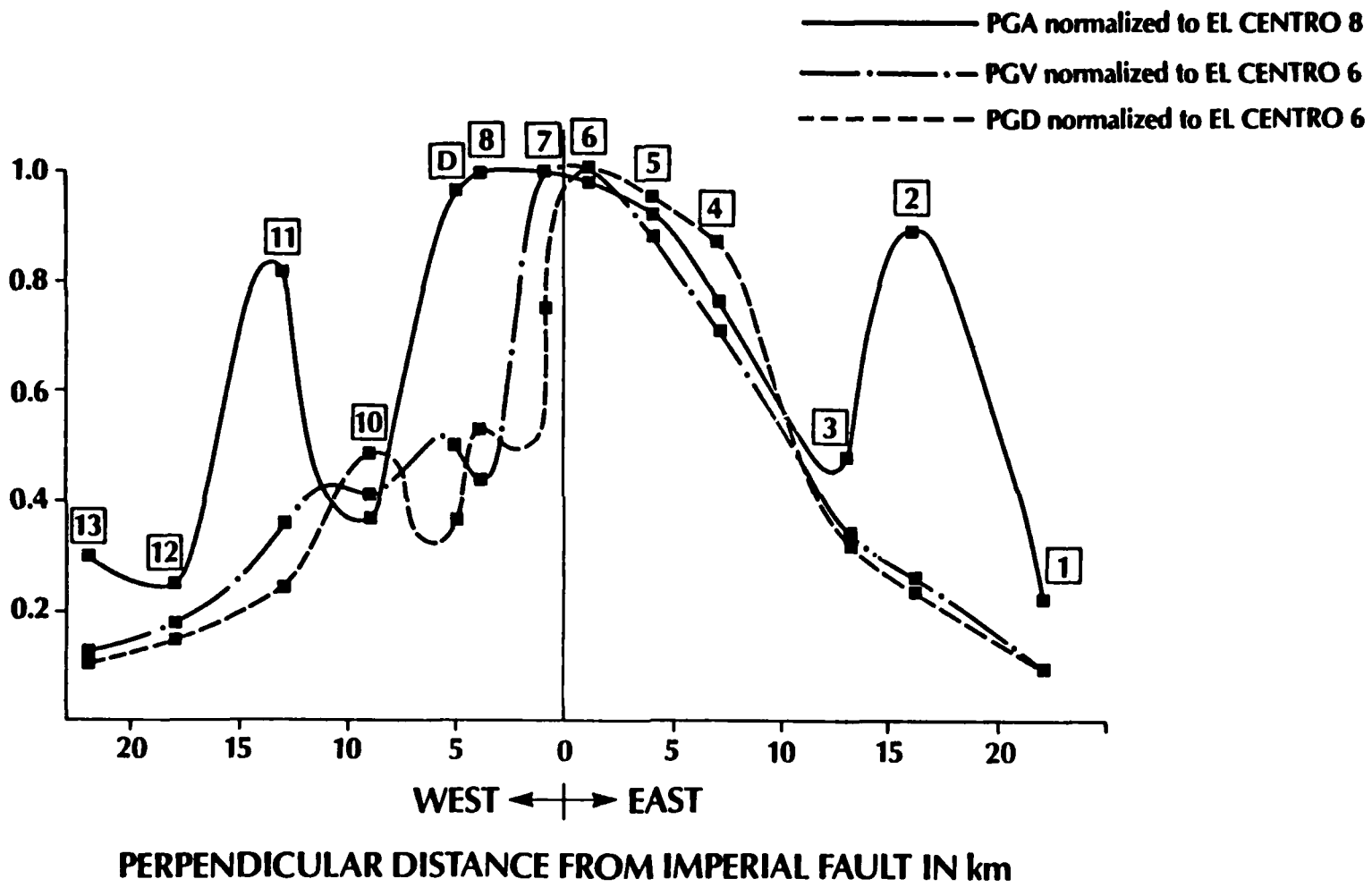

Figure 4.7 Variation of Normalized PGA, PGV and PGD along the El Centro Array (230° Component)

is high and more or less monotonic reaching about one-fifth maximum value at a distance of about 20 km. The PGA curve, by contrast, has a broader central maximum and is tri-modal. Stations 2 and 11 at about 15 km from the ruptured fault show higher accelerations than expected from the average trend. The explanation of these "anomalous" readings could be unusual site soil conditions or unusual surficial crustal properties. Singh (1981) prefers to explain the PGA contours in terms of a diffraction pattern set up by a zone of low-velocity rocks across the fault zone. Seismic refraction data suggest that such a low-velocity seam (see Section 3.4) is over 1 km in width in the basement rocks. The hypothesis is that the high-frequency waves (5-10 Hz) recorded in the accelerograms are damped markedly along the Imperial fault zone, whereas the longer period waves in the velocity and displacement records are showing mainly directivity effects because the channeling and damping effects of the fault seam are not so great at periods of 1 sec and greater.

A final point made by Singh relates to the amplitude spectra of recorded ground motions. Spectral amplitudes for the 230° horizontal component of ground displacement at Stations 6, 7 and Bonds Corner are plotted in Figure 4.8. The spectral envelopes for Stations 6 and 7 (to NW of the rupture) exceed the spectral envelope for Bonds Corner for frequencies less than 0.8 Hz and are less for higher frequencies. This result is in line with the above argument.

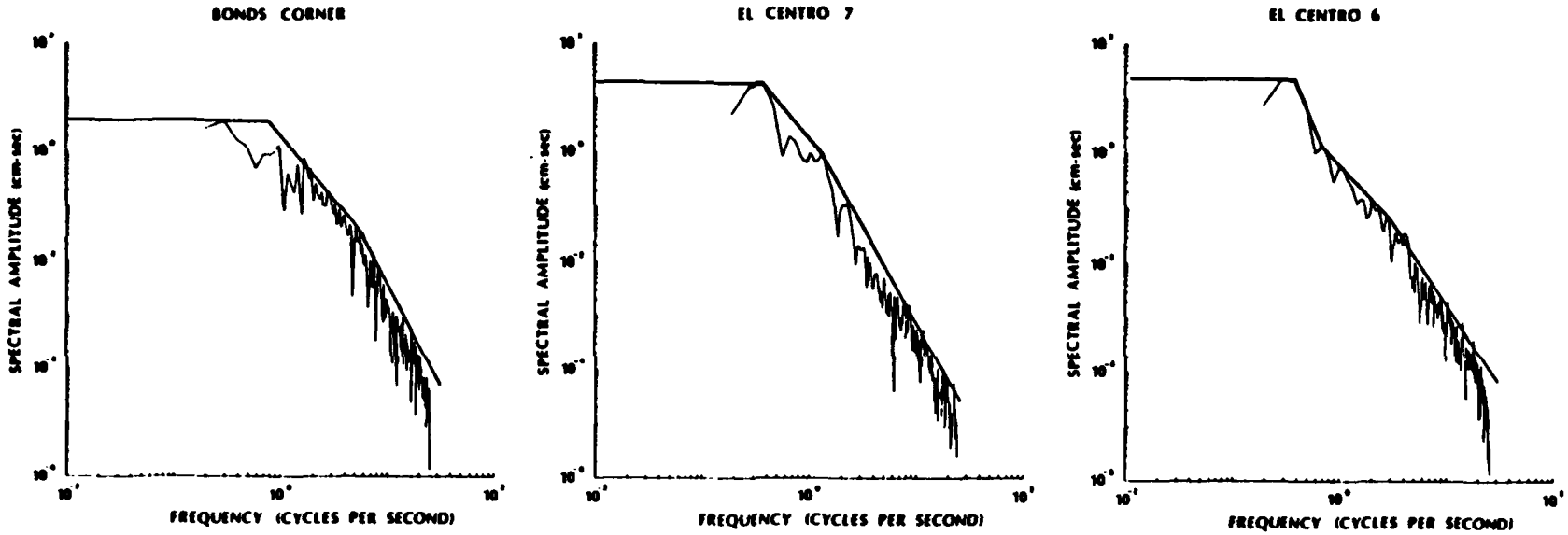

Figure 4.8 Amplitude Spectra and Spectral Envelopes for Shear Wave Displacement Pulse Recorded at Stations El Centro 6, El Centro 7, and Bonds Corner (230° Component)

4.2 Foreign Earthquakes

Descriptions of seismic intensity in a number of earthquakes that have been studied closely in the field outside the United States have led to suggestions of focusing effects. Unfortunately, in many cases, the use of the word "focusing" is not precisely defined. The investigators sometimes have in mind the focusing of waves by variations in underground structures and sometimes the effects of the dynamics of a moving source. One important recent example is the 1977 Romanian earthquake (m_b = 6.8). The isoseismal lines were clearly asymmetric, extending to south and southeast - a pattern (Bolt, 1981) noticed in earlier Romanian earthquakes from the Vrancea zone near the Carpathians.

Another clear example of a great foreign earthquake which produced intensities which probably can best be explained by directivity focusing is the Guatemala earthquake of 4 February 1976. This earthquake was produced by rupture from east to west of the Motagua fault and the isoseismal map is given in Figure 2.1. Modified Mercalli Intensities near Guatemala City and to the north were notably stronger than intensities in the vicinity of Los Amates, with a spreading out of the isoseismal curves. Espinosa (1976) is of the opinion that some geometrical amplification effects of the seismic waves are involved.

As well, there is direct seismological evidence that (at least at long periods) directivity focusing was important in the source mechanism of this earthquake. Espinosa shows the amplitudes of the very long period SH surface waves called G waves which were recorded on long-period seismographs at the WWSSN Station Porto in Portugal. As shown in Figure 4.9, the train of waves, called G2, traveling westward (i.e., in the direction of the source velocity) around the great circle from Guatemala to Porto has a large

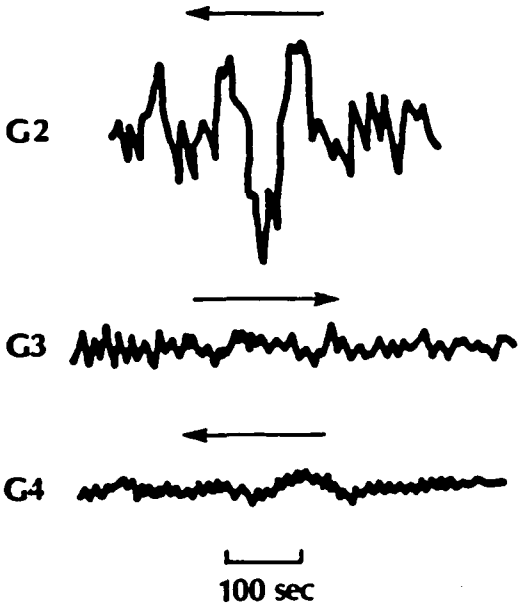

NOTES:

1) Waves G2 and G4 left the source in direction of rupture propagation at an angle of about 15° from the direction of fault rupture.

2) Wave G3 left the source at an angle of about 165° from the direction of fault rupture.

3) Wave G4 has traveled 213° farther than Wave G3.

Figure 4.9 Effect of Source Propagation on G-Wave Amplitudes Recorded at Station Porto, Portugal (from Espinosa, 1976)

hundred-second wave pulse. This pulse is still evident in the wave train called G4 which is produced after the G2 train travels another circuit around the Earth. In comparison, the wave train called G3, which is the SH surface wave pulse that has left the source in the opposite direction to the source propagation, has a virtually undetectable amplitude at Porto.

Specific evidence of directivity focusing has also been given in some seismological studies of Japanese earthquakes. As yet, however, no cases provide evidence of the same strength as the California studies. It is interesting that in his recent book, K. Kasahara (1981), in dealing with the mechanics of earthquakes, discusses directivity focusing as a likely significant phenomenon but does not quote any studies from Japanese earthquakes.

A number of directivity functions have been evaluated in the far field for long-period Love and Rayleigh waves and the results published. These results are consistent with the effectiveness of the term given as equation B-6 in Appendix B. The examples include the great Chilean earthquake of 22 May 1960 and the great Alaskan earthquake of 28 March 1964 (Ben-Menahem and Singh, 1981).

4.3 The Greenville (Livermore) Earthquake Sequence, 24 January 1980

The principal earthquake at $1900^h\ 00^m\ 09.46^s$ UTC on the 24th of January, 1980, with $M_L = 5.5$ at Berkeley, caused a surprising amount of damage north of Livermore Valley and was associated with surface rupture along the Greenville fault (Figure 4.10). There was a foreshock ($M_L = 2.7$) a minute and a half earlier and a sequence of 59 events ($M_L \geq 2.5$) in the ensuing six days. On January 27 at $02^h\ 33^m\ 35.96^s$, a second principal earthquake occurred in the sequence ($M_L = 5.6$ at Berkeley). This second principal shock was located 14 km to the south of the first principal earthquake towards the southern end of the Greenville fault. The location of the earthquake sequence in relation to the Greenville fault and the Livermore Valley in central California is shown in Figure 4.10. The two principal earthquakes, 1/24 and 1/27, are number 2 and 11, respectively.

Preliminary estimates of the seismic moments of the two principal shocks are 5.3×10^{24} and 1.3×10^{24} dyne-cm, respectively. The sequence is of particular interest for the present study for two reasons. First, clear surface faulting was observed on a mapped fault, the Greenville fault, and extended, as observed by cracks in fields and roads, along the strike for at least 6 km. The fault offset was predominately right-lateral but varied from place to place in the soil, sometimes accompanied by comparable vertical offsets with small sag sections common. On the average, the northeast side went up. The location of the focus and aftershocks argue for rupture from north to south along the fault in the 1/24 mainshock.

Secondly, the radiation patterns in intensity for the two principal shocks were clearly different, with the shock of January 27 exhibiting an asymmetrical intensity radiation pattern with larger amplitudes towards the northeast. The first principal earthquake caused damages of various extents

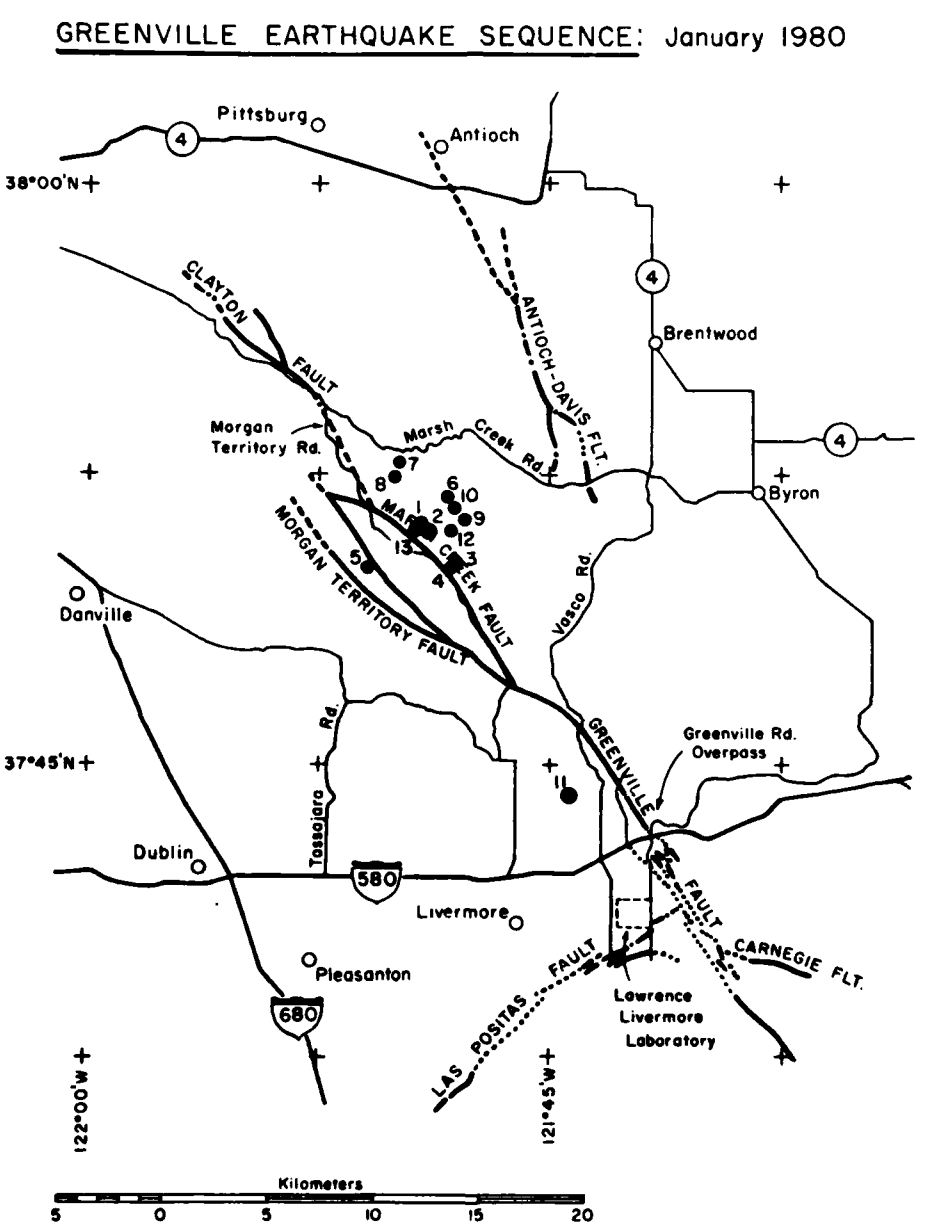

Figure 4.10 Epicenters of Principal Earthquakes in the Greenville Sequence, January 1980

to a few facilities of the Lawrence Livermore National Laboratory. Because of its moderate size (M_L = 5.5), this circumstance caused some surprise and raised questions of the mechanism of the wave generation in this case. The 1/27 principal earthquake had its focus near the south end of the Greenville fault. It produced less intensity in the Livermore area than in towns to the north, i.e., Danville, Concord, and Antioch (although having a focus nearer the former). At the more northerly area, there was a consensus that the 1/27 earthquake was felt more sharply than the first and there was confirmation from minor building damage in Antioch in the 1/27 event that was not paralleled during the 1/24 earthquake (Bolt et al.,1981).

Evidence is also available from instrumental readings. The first set arises in terms of the magnitudes of the two principal shocks. The Wood-Anderson seismograms from which the Berkeley Richter magnitudes were calculated are shown in Figures 4.11 and 4.12. There is no question but that the maximum amplitude recorded by the torsion instrument at Berkeley from the 1/27 earthquake is greater than the maximum trace amplitude from the 1/24 earthquake.

At the Santa Barbara seismographic station, SBC, to the south, by contrast, the 1/24 earthquake produced substantially larger amplitudes on Wood-Anderson seismographs than did the 1/27 shock (see Figure 4.13). In agreement with the other evidence for strong azimuthal variation in radiation, the opposite ratio occurs at the northern California Arcata (ARC) station. It will also be noticed that the wave duration is greater in the case of the first earthquake. A problem for comparisons of magnitude, seismic moment, intensity and so on for this pair of earthquakes is the greater complexity of the first principal shock. This is evident from the recording of three separate peaks (Figure 4.11) indicating multiple events superimposed within

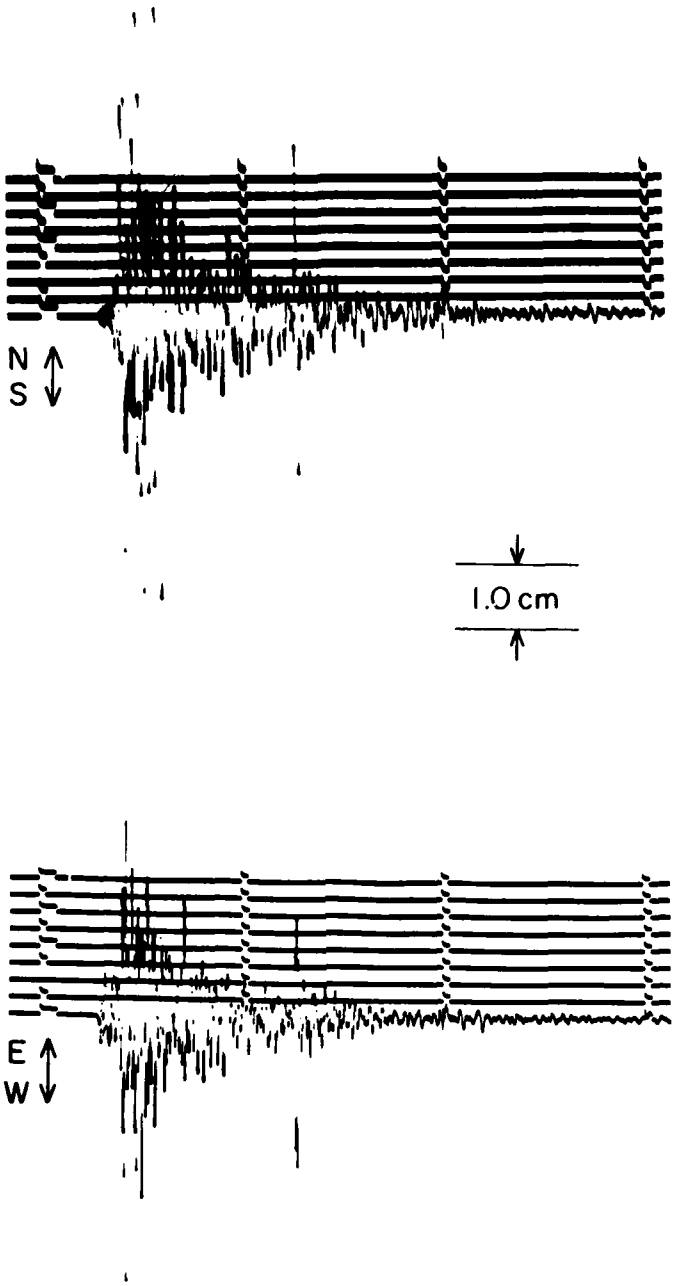

Figure 4.11 Portion of the Berkeley 100 × magnification torsion seismograms showing the duration and amplitudes in the 1/24 principal shock. Distance between time marks is 1 min

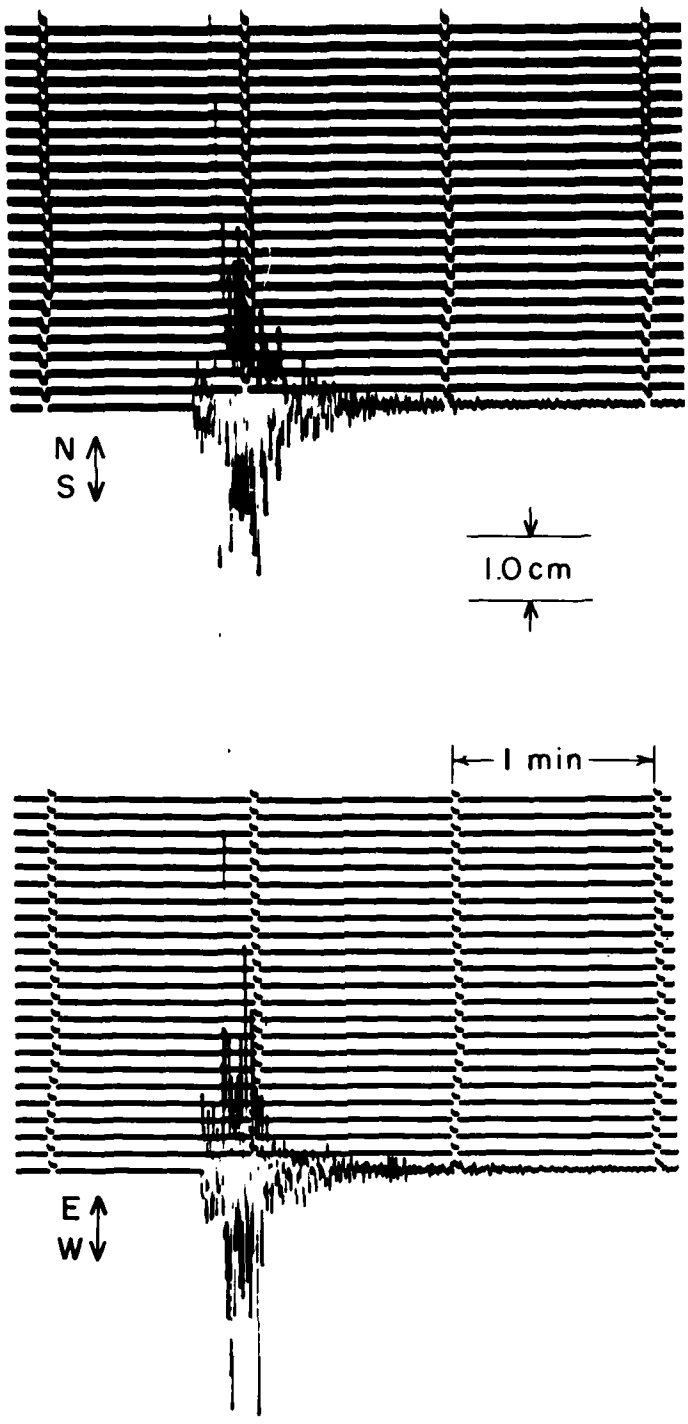

Figure 4.12 Portion of the Berkeley 100 × magnification torsion seismograms for the 1/27 principal shock. Same scale as Figure 4.11. Notice the shorter duration and larger amplitude than in the 1/24 shock as recorded at BRK about 30° further west of the NW strike of the ruptured fault

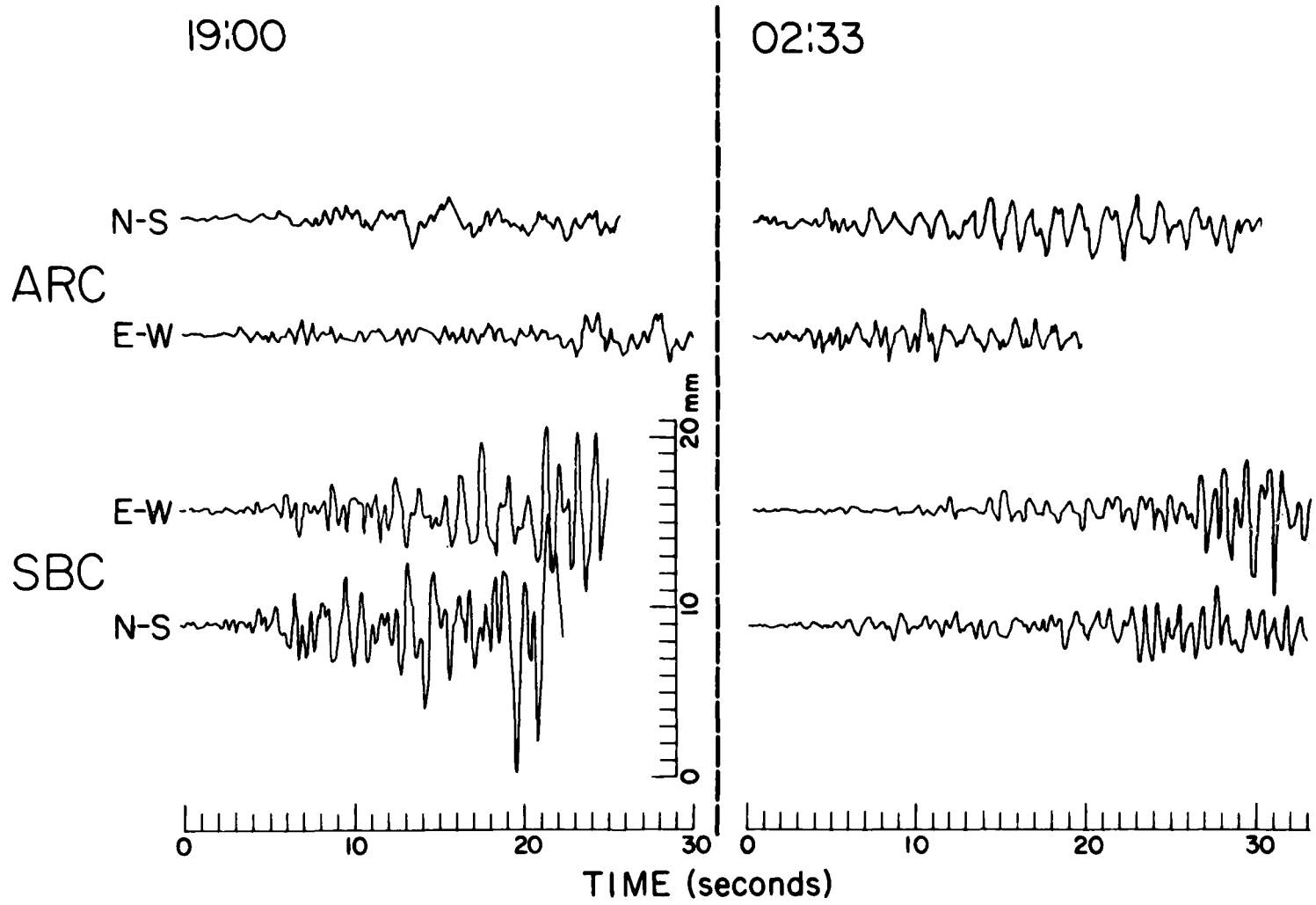

Figure 4.13 Wood-Anderson accelerograms of the 1/24 principal shock (19:00) and the 1/27 principal shock (02:33) recorded at Arcata and Santa Barbara, respectively (after B. Schechter, 1981, personal communication)

about 1 minute. The extended duration in the 1/24 shock has two consequences of importance for the present study. First, the lengthier shaking may have contributed to the damage reported at the Lawrence Livermore National Laboratory area in the first earthquake. Second, the use of duration of coda length for discussions of directivity focusing can be error-prone in the case of multiple shocks.

The mechanisms of the ruptures involved in the two principal shocks can now be summarized. The evidence from the field observations, the hypocentral locations, and the fault plane solutions is that the 1/24 rupture began to the north, causing right-lateral displacement along the northerly extension of the Marsh Creek fault. The rupture then moved along the Greenville strike and proceeded for about 20 km southward, producing surface ruptures, with the faulting ending near Highway 580 overpass at Greenville Road. Such unilateral southern progression of the seismic wave source produced radiation conditions which could have enhanced the strong ground motion at the south end of the faulting and decreased it somewhat to the north. The position of the focus of the 1/27 earthquake near the southern end of the faulting suggests further southward rupture of the Greenville fault. Field evidence, however, indicates no surface faulting south of Highway 580 along the Greenville fault, but some additional displacements along the surface rupture already evident after the 1/24 event. A plausible explanation is that the second earthquake involved northward rupture velocity. If this is the case, this event is an example of a fault dislocation retracking along an earlier path, either through or above or below the earlier rupture. The depths of the two principal foci of 11.8 and 14.5 km suggest deep crustal rupture planes with only limited expression on the surface.

The radiation of ground horizontal peak accelerations, velocities and energy flux in the 1980 Livermore Valley earthquakes has been subject to a close analysis in a recent paper by Boatwright and Boore (1982). These authors examine the strong-motion accelerograph recordings at 27 stations within about 60 km of the 1/24 mainshock and the 1/27 shock for systematic variations which might be indicative of either site effects or directivity. They find that the variation of peak accelerations with azimuth relative to the source is reversed for the two events and agree with the intensity information that the mainshock accelerations are larger to the southeast, whereas the second principal shock accelerations are larger to the northwest. They have eliminated the site effects by forming the ratios of the peak accelerations from the two events and this process indicates that the source directivity in this case caused a total variation of up to a factor of about 5 in the peak accelerations. The key observational comparison is given in Figures 4.14 and 4.15. They find that the simple application of the directivity function given by equation (3.1) fits the acceleration data well for a reasonable rupture velocity. They find also a similar but smaller azimuthal variation in peak velocities and radiated seismic energy.

It should be pointed out, however, that the effect of the directivity in this case is being measured at some distance from the source itself and with accelerations that are smaller (generally less than 0.1g) than those of engineering interest. In the 1/24 shock, all but one station had a distance greater than 15 km from the fault source trace . In the 1/27 principal earthquake, all but 3 stations had distances greater than 10 km from the source; in this case two additional stations recorded at distances of 4 and 8 km from the source, with azimuths of 246° and 314°, and peak

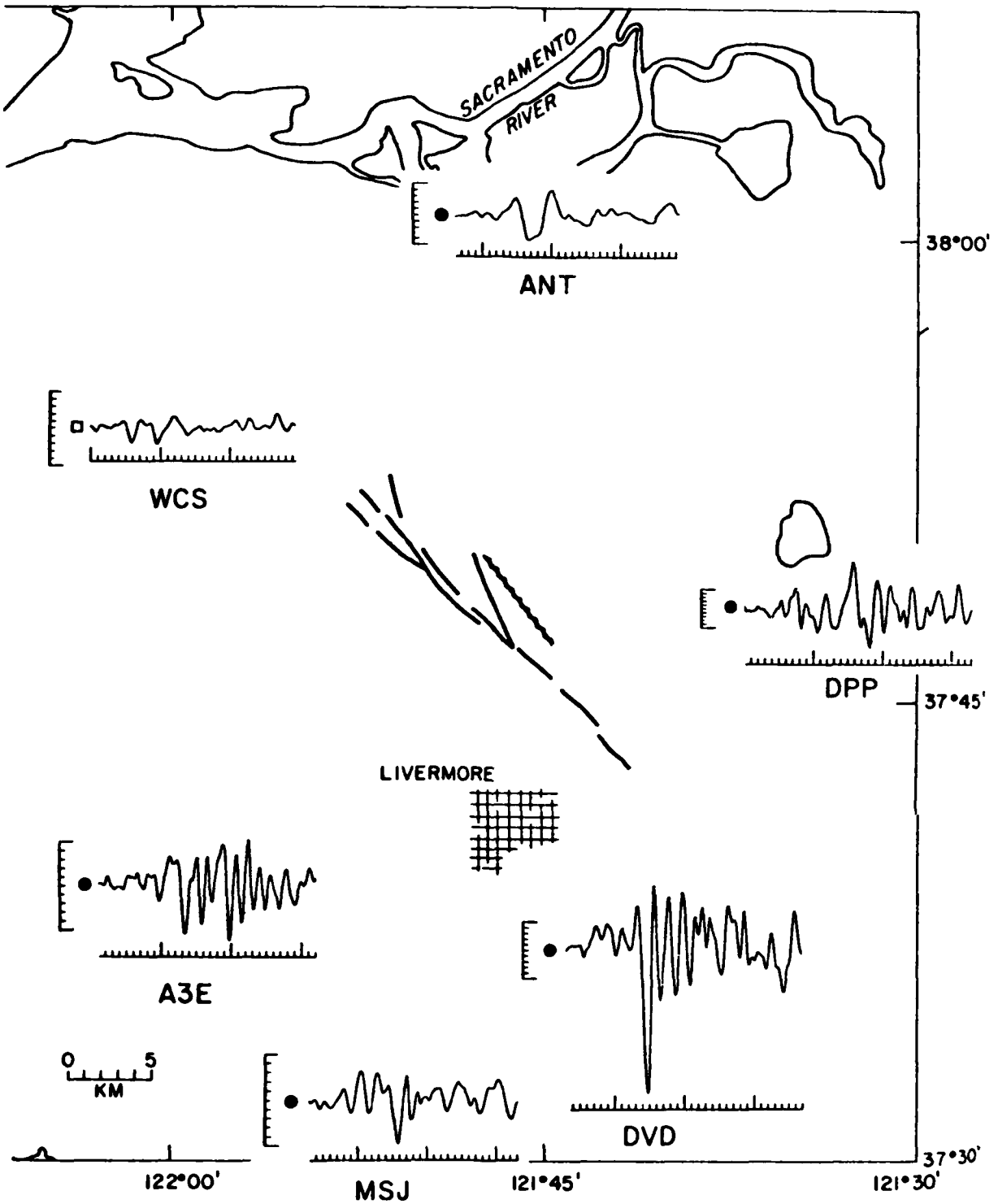

Figure 4.14 Selected SH accelerograms of the 1/24 mainshock superimposed on a map of the Livermore area, showing the directivity in peak motions and relative complexity of the mainshock accelerograms. The acceleration scales have been adjusted to compensate for the expected 1/R geometrical spreading; each scale has 100 cm/sec^2 between the large tick marks. (After Boatwright and Boore, 1982)

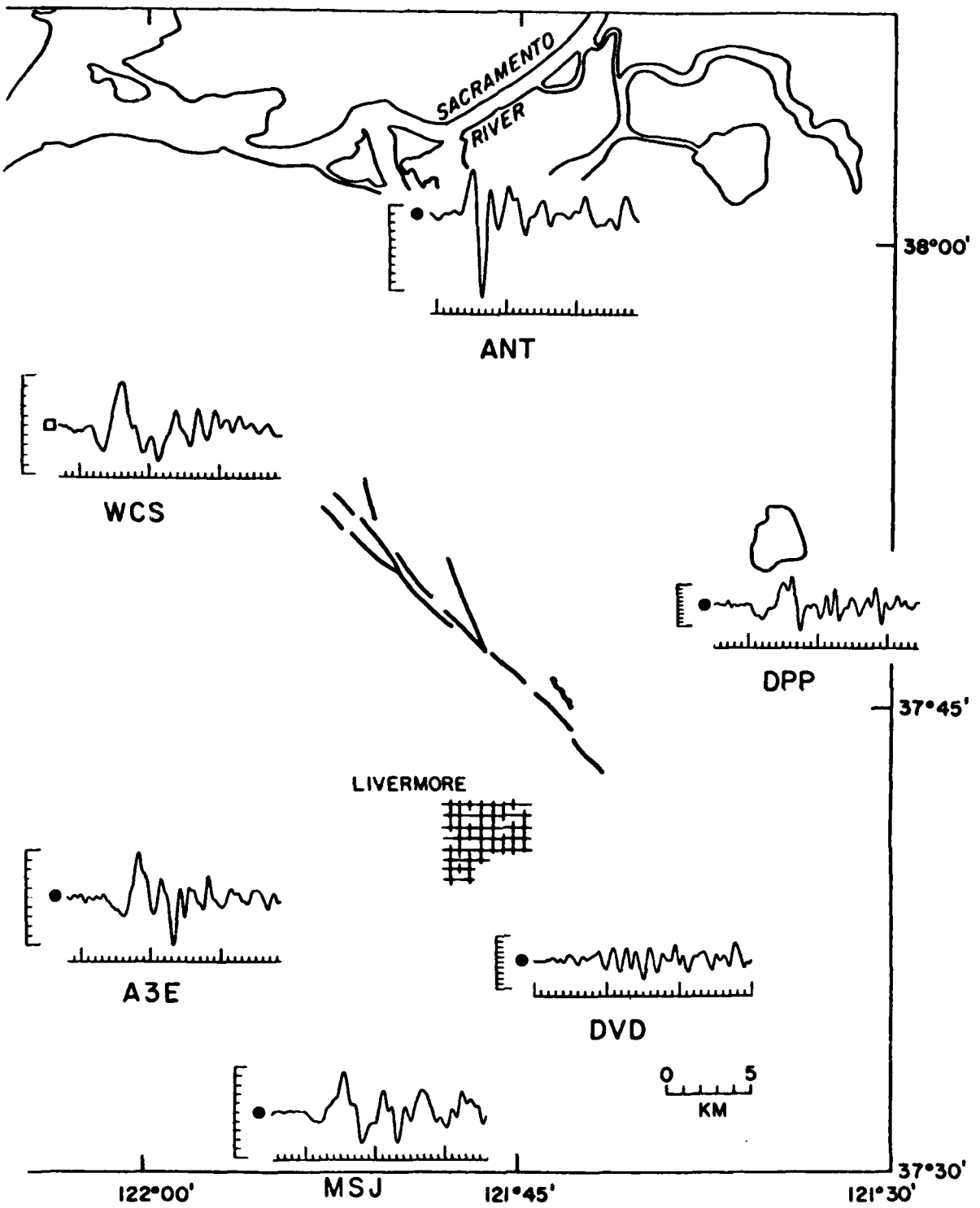

Figure 4.15 Selected SH accelerograms of the 1/27 aftershock. The acceleration scales have been adjusted as in Figure 4.14. Note the strong amplification to the northwest, relative to the 1/24 accelerograms

accelerations of 0.26g and 0.27g, respectively. Unfortunately, the nearest strong-motion station is at an azimuth which would have high SH motions for right-lateral strike-slip rupture independently of directivity rupture considerations. The recorded data also show a few anomalous points, particularly in PGV. The data, moreover, do not directly measure the effective directivity in a narrow lobe along the fault zone. They do show that a moving dislocation effect is able to explain the amplitudes of predominately SH wave motions at distances greater than about 25 km better than a static (double-couple) source. The evidence is, however, the most persuasive to date for significant directivity focusing contributions at distances of a few tens of kilometers from the fault source of moderate earthquakes.

PART V

FINAL ANALYSES

5.1 General Conclusions

At the present stage of strong-motion studies there still remains considerable uncertainty regarding the extent and effectiveness of directivity focusing in modifying strong ground shaking. Nevertheless, a number of general conclusions can be drawn.

First, from a seismological point of view, the effect of the moving source has been clearly demonstrated in numerous studies using seismographs located at both moderate and great distances (i.e., the far field) from the source. Such studies, however, usually concern long-period seismic waves with periods above 2 to 5 seconds. Secondly, when seismic waves in the near field with a range of wave frequencies characteristic of engineered structures (i.e., 1 Hz to 10 Hz) are considered, there is as yet only limited definitive evidence available, and this is somewhat contradictory. Nevertheless, the likelihood is that directivity focusing in strong motion is limited in the near field, but that the elementary predictions of the magnitude of the effects can be sometimes modified or even overwhelmed by other features of the source mechanism, the geological variations along the wave paths and within the fault zone.

Thirdly, the ratio of peak horizontal ground motion in the forward direction of fault rupture to the peak motion in the backwards direction is probably greatest for ground displacements and velocities and least for peak accelerations. High-frequency ground accelerations show variations due to scattering, attenuation, and source asperities that mask directivity effects.

It is necessary to make some summary comments concerning the inferences of Singh (1981) for the 1979 Coyote Lake and 1979 Imperial Valley earthquakes (see Section 4.1) and the evaluation of Boatwright and Boore (1982) for the 1980 Livermore earthquakes (see Section 4.3). Singh was among the first to demonstrate from strong-motion accelerometer records the reality of directivity focusing in the geotechnical context. He found that the effect was frequency-sensitive. His analysis of the strong-motion records available to him suggested that peak ground acceleration (high-frequency) was affected by directivity less than peak velocity (intermediate frequency) and peak displacement (low frequency). The contours of peak ground acceleration for the Imperial Valley earthquake were complicated and did not resemble in certain ways the predicted contours for a simple moving source, and he pointed out that the peak accelerations obtained at two stations closely adjacent to the Imperial fault were opposite to that predicted by the simple model of directivity focusing.

By comparison, Boatwright and Boore inferred a factor of 5 in acceleration focusing in the azimuth of the propagating dislocation along the Greenville fault. It has been pointed out (Section 4.3), however, that in the mainshock crucial strong-motion instrumentation was not available close to and along the strike of the Greenville fault, but at various azimuths at distances beyond 15 km from the seismic source. Boatwright and Boore were therefore required to interpolate the available measurements (see, e.g., Figure 4.14). Finally, a few stations in the case of the Livermore earthquakes did not have recorded accelerograms in agreement with the overall radiation patterns. The meaning of these anomalies from the predicted wavefield has not as yet been explored.

In summary, recordings of ground motion in three moderate California earthquakes of 1979 and 1980 provide positive evidence for a measurable effect of dislocation velocity along the rupturing fault on recorded strong ground motions. The consequences are superimposed on independent effects arising from complex source mechanisms, propagation path complications, and site condition variability.

5.2 Engineering Implications for Site Evaluations

As summarized in Section 5.1, the evidence presented in this report indicates that directivity focusing of seismic waves from a moving fault rupture has been confirmed in a general way. The main effect is to distort the wave radiation patterns that occur for static double-couple force systems. Because, however, most strong-motion parameters are averages of samples of measurements obtained under various circumstances, with variable distances, source properties, geological conditions and azimuth from the seismic source; moving source effects are included in the estimates of means and variances.

Because of the various complexities concerning a particular site and candidate capable faults or modes of faulting in its vicinity, quantitative incorporation of a directivity factor in site-specific strong-motion parameter estimates cannot be recommended at this time. Although there is strong evidence from the field instrumental measurements in the 1979 Imperial Valley, the 1979 Coyote Lake, and the 1980 Greenville (Livermore) earthquakes for directivity focusing effects, the actual direction of the moving source cannot be predicted. Therefore a site may be on the high or low side of the radiation wave field. The use of averages of all relevant recorded motions will, moreover, always incorporate the directivity effect, at least in the sense of ground motions with the greatest expectation.

For example, in the testimony before the Atomic Safety and Licensing Appeal Board on the Diablo Canyon Nuclear Power Plant site (see Section 2.1), comments were made on directivity focusing. It was generally agreed that the effects of focusing are generally included in the seismic analysis,

but that it might explain some observed scatter of peak acceleration, velocity, and so on. Furthermore, the concept of seismic focusing was characterized as generally theoretical in substance and still speculative. Testimony indicated that the effects of focusing occur in every earthquake to some degree for sites where there is propagation in the direction of the instrument. For this reason, the strong-motion earthquake recordings take into account on the average the effects of seismic focusing. The difficulty is that for any given earthquake on the Hosgri fault it is now not possible to predict whether it would focus energy towards or away from the Diablo Canyon site. There was testimony that, for large earthquakes, accelerations may theoretically reach 2g but that, to date, in only two cases were horizontal accelerations greater than 1g measured. In fact, no witness was able to assign a probability to the likelihood that given seismic focusing effects would be associated with ground motion at the Diablo Canyon site.

Because seismic focusing is a special near-field earthquake ground motion effect which may be experienced at a site towards which fracture propagation progresses, local amplification of the ground motion might arise. The effect should, therefore, be considered in shaking estimates for critical structures such as dams, bridges, power plants, etc., because such focusing can significantly increase the spectral components of ground motion employed as input into the seismic design.

A final relevant point for geotechnical studies is that modern assessments of near-field strong ground motions usually include elements which generally take account of the dynamics of fault rupture. It is now good practice to include at an appropriate portion of a near-source

record a longer period pulse which corresponds to the elastic rebound or "fling" along the the fault as the dislocation passes by the site (see Bolt, 1981). This fling ensures for most engineering purposes that the longer period parts of the response spectrum are realistically energetic.

5.3 Future Research

The general survey and discussion in the previous sections have brought to light a number of important avenues of work for the future. First, intensity studies can be of value in making assessments of the practical consequences of aspects of the earthquake generation process. For example, the detailed field evidence of intensities along the ruptured fault in both the 1906 earthquake and the 1952 Kern County earthquake along the White Wolf fault are most important correctives to the view that structures are most heavily shaken along the fault itself. In future earthquakes where surface faulting is observed and the requisite elements for intensity assessments exist, every effort should be made to make detailed accounting of damage and other shaking parameters. In this respect, some reassessment of the calibration of the Modified Mercalli intensity scale is probably required. In particular, it would be most helpful to incorporate more of what is now known about the effect of soils on attenuation. In this respect, contributions of soils engineers in re-assessments of intensities and reconstruction of the intensity scale would be valuable.

Secondly, it is clear that a significant advance in knowledge of directivity focusing effects depends on the installation and maintenance of strong-motion accelerometers along active faults where large earthquakes might be generated. As the studies described in the previous sections have shown, there are still only a handful of accelerograms from moderate to large earthquakes that allow comparisons at the front and back of a moving source dislocation.

In order to achieve the instrumental requirements, specially designed digital instrument arrays must be installed along active fault zones.

These arrays can be designed to give the quantitative detail necessary to model properly the intricacies of strong ground motion near to a source moving through a geologically realistic medium.

On the theoretical side, the discussion has demonstrated that more appropriate theoretical models must be used in examining the quantitative effect of directivity focusing in the frequency ranges of interest in hazard assessment and for engineering design purposes. The application of finite element methods to the complete problem promises to allow the introduction of vertical fault zones or seams in the country rock having more realistic seismic properties. In the meantime, predictions of strong ground motion at high frequences based upon simple theoretical models that do not incorporate adequate variations in gradients in structural and elastic properties and wave damping must be viewed with caution.

REFERENCES

Aki, K., and P.G. Richards (1980). Quantitative Seismology, Theory and Methods, W.H. Freeman and Company, San Francisco, Vol. II.

Archuleta, R.J. (1979). Rupture propagation effects in the Coyote Lake earthquake (abs), EOS (Trans. Am. Geophys. Un.), 60, 890.

Bakun, W.H., R.M. Stewart, and C.G. Bufe (1978). Directivity in the high-frequency radiation of small earthquakes, Bull. Seism. Soc. Am., 68, 1253-1263.

Benioff, H. (1955). Mechanism and strain characteristics of the White Wolf fault as indicated by the aftershock sequence, Earthquakes in Kern County, California during 1955 (G.B. Oakeshott, ed.), Cal. Div. Mines Bull. 171, 199-202.

Ben-Menahem, A., and S.J. Singh (1981). Seismic Waves and Sources, Springer-Verlag, New York.

Boatwright, J., and D.M. Boore (1982). Analysis of the ground accelerations radiated by the 1980 Livermore Valley earthquakes for directivity and dynamic source characteristics, U.S. Geol. Survey Open File Report 82-591.

Bolt, B.A. (1972). San Fernando rupture mechanism and the Pacoima Dam strong motion record, Bull. Seism. Soc. Am., 62, 1053-1061.

Bolt, B.A. (1981). Interpretation of strong motion records, U.S. Army Engineer Waterways Experiment Station, Vicksburg, Mississippi, Report 17.

Bolt, B.A., T.V. McEvilly, and R.A. Uhrhammer (1981). The Livermore Valley, California sequence of January 1980, Bull. Seism. Soc. Am., 71, 451-463.

Brady, A.G., V. Perez, and P.N. Mork (1980). The Imperial Valley earthquake, October 15, 1979, Seismic Engineering Report, U.S. Geol. Survey Open File Report 80-703.

Brune, J.N. (1978). Contention 3 Ground Motion, Testimony on behalf of Intervenors before USNRC Atomic Safety and Licensing Board in matter of Diablo Canyon Nuclear Power Plants, Units 1 and 2, Docket Nos. STN 50-275, 50-323.

Burridge, R. and F. J. Sabina (1972). The propagation of elastic surface waves guided by ridges, Proc. Roy. Soc. A. 330, 417-441.

Drake, L.A. and M.W. Asten (1982). Wave Propagation in Irregular Coal Seams (Manuscript, private communication), pp. 1-5.

Espinosa, A.F. (1981). Attenuation of strong horizontal ground accelerations in the West United States and their relation to M_L, Bull. Seism. Soc. Am., 70, 583-616.

Filson, J., and T.V. McEvilly (1967). Love wave spectra and the mechanism of the 1966 Parkfield sequence, Bull. Seism. Soc. Am., 57, 1245-1259.

Hanks, T.C., and R.K. McGuire (1981). The character of high-frequency strong ground motion, Bull. Seism. Soc. Am., 71, 2071-2096.

Heaton, T.H., and D.V. Helmberger (1979). Generalized ray models of the San Fernando Earthquake, Bull. Seism. Soc. Am., 69, 1311-1341.

Kasahara, K. (1981). Earthquake Mechanics, Cambridge University Press.

Krey, T.C. (1963). Channel waves as a tool of applied geophysics in coal mining, Geophysics, 28, 701-714.

McGuire, R.N., and T.C. Hanks (1980). RMS accelerations and spectral amplitudes of strong ground motion during the San Fernando, California earthquake, Bull. Seism. Soc. Am., 70, 1907-1919.

Morse, P.M., and K.V. Ingard (1968). Theoretical Acoustics, McGraw-Hill Book Company, New York.

Richter, C.F. (1958). Elementary Seismology, W.H. Freeman, San Francisco.

Singh, J.P. (1981). The influence of seismic source directivity on strong ground motions, Ph.D. Dissertation, U.C. Berkeley.

Uhrhammer, R.A. (1980). Observations of the Coyote Lake, California earthquake sequence of August 6, 1979, Bull. Seism. Soc. Am., 70, 559-570.

BIBLIOGRAPHY

Aki, K. (1968). Seismic displacements near a fault, Jour. Geophys. Res., 73, 5359-5376.

Anderson, T. (1974). A dislocation model for the Parkfield earthquake, Bull. Seism. Soc. Am., 64, 671-686.

Archuleta, R.J., and J.N. Brune (1975). Surface strong motion associated with a stick-slip event in a foam rubber model of earthquakes, Bull. Seism. Soc. Am., 65, 1059-1071.

Archuleta, R.J., and G. Frazier (1978). Three-dimensional numerical simulations of dynamic faulting in a half-space, Bull. Seism. Soc. Am., 68, 541-572.

Ben-Manahem, A. (1961). Radiation patterns of seismic surface waves from finite moving sources, Bull. Seism. Soc. Am., 51, 401-435.

Bolt, B.A. (1973). Duration of strong ground motion, Proc. Fifth World Conference on Earthquake Engineering, Rome, Italy, 1, 1304-1313.

Boore, D.M. (1973). Empirical and theoretical study of near-fault wave propagation, Proc. Fifth World Conference on Earthquake Engineering, Rome, Italy, 2, 2397-2408.

Boore, D.M., and M.D. Zobach (1974a). Near field motions from kinematic models of propagating faults, Bull. Seism. Soc. Am., 64, 321-342.

Boore, D.M., and M.D. Zobach (1974b). Two-dimensional kinematic fault modeling of the Pacoima Dam strong motion recordings of February 9, 1971, San Fernando earthquake, Bull. Seism. Soc. Am., 64, 555-570.

Borcherdt, R.D. (1970). Effects of local geology on ground motion near San Francisco Bay, Bull. Seism. Soc. Am., 60, 29-61.

Brady, A.G., P.N. Mork, V. Perez, and L.D. Porter. Processed data from the Gilroy array and Coyote Creek records, Coyote Lake, California earthquake August 6, 1979, U.S. Geol. Survey Open File Report 81-42.

Brune, J.N. (1970). Tectonic stress and the spectra of seismic shear waves from earthquakes, Jour. Geophys. Res., 75, 4997-5009.

Brune, J.N. (1970). Correction. Tectonic stress and the spectra of seismic shear waves from earthquakes, Jour. Geophys. Res., 76, 5002.

Brune, J.N. (1973). Earthquake modelling by stick-slip along pre-cut surfaces in stressed foam rubber, Bull. Seism. Soc. Am., 63, 2105-2119.

Brune, J.N. (1976a). The Physics of Earthquake Strong Motion in Seismic Risk and Engineering Decisions, C. Lomnitz and E. Rosenblueth (eds.), Elsevier Science Publication Company, New York.

Brune, J.N. (1976b). Letter to Executive Director, Advisory Commission on Reactor Safeguards, Nuclear Regulatory Commission, Washington, D.C. explaining the phenomenon of high energy focussing by propagating earthquake rupture and its possible relevance to the Diablo Canyon Nuclear Power plant.

Brune, J.N. (1977). Statement to Advisory Commission on Reactor Safeguards in matter of Diablo Canyon Nuclear Power Plants, Units 1 and 2.

Brune, J.N., and C. Lomnitz (1974). Recent seismological developments relating to earthquake hazard, Geofis. Int., 14, 49-63.

Cannitz, N., and M.N. Toksoz (1972). Static and dynamic study of earthquake source mechanism, San Fernando earthquake, Jour. Geophys. Res., 77, 2583-2594.

Duke, C.M., R.T. Eguchi, K.W. Campbell and A.W. Chow (1976). Effects of site on ground motions in the San Fernando earthquake, Report No. UCLA-ENG 7688, University of California, Los Angeles, August.

Espinosa, A.F. (1976). The Guatemalan earthquake of February 4, 1976. A preliminary report, U.S. Geol. Survey Professional Paper 1002.

Espinosa, A.F. (1980). M_L and M_o determination from strong motion accelerograms and expected intensity distribution, U.S. Geol. Survey Open File Report 80-1094, C. Rojahn (ed.).

Gutenberg, B. (1955). Magnitude determination of larger Kern County shocks, 1952; Effects of station azimuth and calculation methods, Cal. Div. Mines Bull. 171, 171-175.

Gutenberg, B. (1957). Effects of ground on earthquake motion, Bull. Seism. Soc. Am., 47, 221-250.

Hanks, T.C., J.A. Hileman, and W. Thatcher (1975). Seismic moments of the larger earthquakes of the Southern California region, Geol. Soc. Am. Bull., 86, 1131-1139.

Hanks, T.C., and D.A. Johnson (1976). Geophysical assessment of peak accelerations, Bull. Seism. Soc. Am., 66, 959-968.

Hanson, M.E., A.R. Sanford and R.J. Shaffer (1974). A source function for dynamic brittle unilateral shear fracture, Geophysical Journal of the Royal Astronomical Society, 38, 365-376.

Hartzell, S.H., G.A. Frazier and J.N. Brune (1978). Earthquake modeling in a homogeneous half-space, Bull. Seism. Soc. Am., 68, 301-316.

Hartzell, S.H., and R.J. Archuleta (1979). Rupture propagation and focussing of energy in a foam rubber model of stick-slip earthquake, Jour. Geophys. Res., 84, 3623-3636.

Haskell, N.A. (1964). Total energy and energy spectral density of elastic wave radiation from propagating faults, Bull. Seism. Soc. Am., 54, 1811-1841.

Haskell, N.A. (1966). Total energy and energy spectral density of elastic wave radiation from propagating faults, II, Bull. Seism. Soc. Am., 56, 125-140.

Haskell, N.A. (1969). Elastic displacements in the near field of a propagating fault, Bull. Seism. Soc. Am., 59, 865-908.

Heaton, T.H. and D.V. Helmberger (1978). Predictability of strong ground motion in the Imperial Valley: Modelling the M4.9, November 4, 1976 Brawley earthquake, Bull. Seism. Soc. Am., 68, 31-48.

Idriss, I.M. (1978). Characteristics of earthquake ground motion, state-of-the-art report, Proc. ASCE Geotechnical Engineering Division Specialty Conference, June 19-21, Pasadena, Calif., III, 1151-1265.

Jeffreys, H. (1931). On the cause of oscillatory movement in seismograms, Monthly Notices of the Royal Astronomical Society, Geophysical Supplement II, No. 8, 407-441.

Joyner, W.B., and A.T.F. Chen (1975). Calculation of nonlinear ground response in earthquakes, Bull. Seism. Soc. Am., 65, 1315-1336.

Joyner, W.B. and D.M. Boore (1981). Peak horizontal acceleration and velocity from strong-motion records including records from the 1979 Imperial Valley, California earthquake, Bull. Seism. Soc. Am., 71, 2011-2038.

Kanamori, H. (1974). Long-period ground motion in the epicentral area of major earthquakes, Tectonophysics, 21, 341-356.

Kanamori, H., and D.L. Anderson (1975). Theoretical basis of some empirical relations in seismology, Bull. Seism. Soc. Am., 65, 1073-1095.

Kanamori, H., and P.C. Jennings (1978). Determination of local magnitude M_L from strong motion accelerograms, Bull. Seism. Soc. Am., 68, 471-485.

Knopoff, L., and F.A. Gilbert (1959). Radiation from a strike-slip fault, Bull. Seism. Soc. Am., 49, 163-178.

Kostrov, B.V. (1964). Self-similar problems of propagation of shear cracks, Jour. Appl. Math. Mech., 28, 1077.

Lamb, H. (1904). On the propagation of tremors over the surface of an elastic solid, Philosophical Transactions of Royal Society of London, A203, 1-42.

Lamb, H. (1916). On-waves due to traveling disturbance, Phil. Mag., 13, 386-399, and 13, 539-548.

Lee, W., D.G. Herd, V. Cagnetti, W.H. Bakun and A. Rapport (1979). A preliminary study of the Coyote Lake earthquake of August 6, 1979 and its major aftershocks, U.S. Geol. Survey Open File Report 79-1621.

Maruyama, T. (1963). On the force equivalent of dynamic elastic dislocations with reference to the earthquake mechanism, Bulletin Earthquake Research Institute, Tokyo University, 41, 467-486.

McGarr, A. (1981). Analysis of peak ground motion in terms of a model of inhomogeneous faulting, Jour. Geophys. Res., 86, 3901-3912.

McGuire, R.K. (1978). Seismic ground motion parameter relations, Journal of the Geotechnical Division, ASCE, 104, No. GT 4, 481-490.

McJunkin, R.D., and J.T. Ragsdale (1980). Strong-motion records from the Livermore earthquake of 24 and 26 January 1980, Cal. Div. Mines and Geology Preliminary Report 28.

Mohraz, B. (1976). A study of earthquake response spectra for different geological conditions, Bull. Seism. Soc. Am., 66, 915-936.

Morse, P.M. and H. Feshbach (1953). Methods of Theoretical Physics, Part II, McGraw-Hill Book Company, New York.

Porcella, R.L., and R.B. Matthiesen (1979). Preliminary summary of the U.S. Geological Survey strong motion records from the October 15, 1979 Imperial Valley earthquake, U.S. Geol. Survey Open File Report 79-1654.

Porcella, R.L., R.B. Matthiesen, R.D. McJunkin and J.T. Ragsdale (1979). Compilation of strong motion records from the August 6, 1979 Coyote Lake earthquake, U.S. Geol. Survey Open File Report 79-385.

Reagor, B.G., C.W. Stover, S.T. Algermissen, K.V. Steinbrugge, P. Hubiak, M.G. Hopper and L.M. Barnhard (1980). Preliminary evaluation of the distribution of intensity, U.S. Geol. Survey Open File Report 80-1094, C. Rojahn (Ed.).

Richards, P.G. (1973). The dynamic field of a growing plane elliptical shear crack, International Journal of Solids and Structures, 9, 843-861.

Richter, C.F. (1958). Elementary Seismology, W.H. Freeman, San Francisco.

Rojahn, C. (1980). Selected papers in the Imperial Valley, California earthquake of October 15, 1979, U.S. Geol. Survey Open File Report 80-1094.

Savage, J.C. (1965). The stopping phase on seismograms, Bull. Seism. Soc. Am., 55, 47.

Schechter, B. (1981). Source parameters and directivity of the Livermore earthquakes of 1980 (abs.), Earthquake Notes, 52, 83.

Seed, H.B., Ugas and J. Lysmer (1976). Site-dependent spectra for earthquake resistant design, Bull. Seism. Soc. Am., 66, 221-243.

Seed, H.B., R. Murarka, J. Lysmer and I.M. Idriss (1976). Relationships of maximum accelerations, maximum velocity, distance from source and local site conditions for moderately strong earthquakes, Bull. Seism. Soc. Am., 66, 1323-1342.

Sezawa, K. (1929). Generation of Rayleigh waves from a sheet of internal sources, Bulletin Earthquake Institute, Tokyo University, 7, 417-435.

Singh, J.P. (1981). Source directivity and its role in estimation of strong ground motion. A paper presented at the Annual Seismological Society of America meeting held at Berkeley, California, March 23-25, Abstract.

Swanger, H.J., S.M. Day, J.R. Murphy and R. Guzman (1981). State-of-the-art study concerning near-field earthquake ground motion, U.S. Nuclear Reg. Comm., NUREG/CR-1978.

Switzer, J., D. Johnson, R. Maley and R. Matthiesen (1981). Western hemisphere strong-motion accelerograph station list - 1980, U.S. Geol. Survey Open File Report 81-664.

Trifunac, M. and J.N. Brune (1970). Complexity of energy release during the Imperial Valley, California earthquake of 1940, Bull. Seism. Soc. Am., 60, 137-160.

Trifunac, M. and F. Udwadia (1974). Parkfield, California earthquake of June 27, 1966: A three-dimensional moving dislocation, Bull. Seism. Soc. Am., 64, 511-534.

Trifunac, M.D., and A.G. Brady (1975). On the correlation of seismic intensity scales with the peaks of recorded strong ground motion, Bull. Seism. Soc. Am., 65, 139-162.

Trifunac, M.D., and J.G. Anderson (1977). Preliminary empirical models for scaling absolute acceleration spectra, Report No. CE77-02, Department of Civil Engineering, University of Southern California, Los Angeles, August.

Tsai, B.Y., and H. Patton (1973). Interpretation of the strong motion earthquake accelerograms using a moving dislocation model. The Parkfield, California earthquake of June 28, 1966. 68th Annual Meeting Seismological Society of America, Golden, Colorado. Abstract.

Ulrich, F.P. (1941) The Imperial Valley earthquake of 1940, Bull. Seism. Soc. Am., 31, 13-31.

Wu, F.T. (1968). Parkfield earthquake of June 28, 1966: Magnitude and source mechanism, Bull. Seism. Soc. Am., 58, 689-709.

Wu, F.T., K.C. Thompson and H. Kuenzler (1972). Stick-slip propagation velocity and seismic source mechanism, Bull. Seism. Soc. Am., 62, 1621.

Wyss, M., and J.N. Brune (1967). The Alaska earthquake of March 28, 1964: A complex multiple rupture, Bull. Seism. Soc. Am., 57, 1017-1023.

APPENDIX A

GEOMETRICAL CONSTRUCTION FOR RUPTURE IN A LOW VELOCITY FAULT ZONE

When a vertical (say) fault zone is taken into account in modeling the seismic wave field from a moving dislocation, computation of the field becomes more complicated than in the simple single fault-plane model. Solutions for the seismic wave equation for boundary conditions appropriate for such a geometry do not appear to be available in the literature (see Section 3.4), although some finite element modeling of these conditions has been started by the author.

It is of some value, however, to give an elementary picture of the effect of the fault zone (or seam) by means of a family of wave fronts. Consequently, in Figure A.1, a modification of the well-known effect of a subsonic unidirectional moving point source is presented for comparison with Figure 3.3. (The interesting case of a rupture supersonic in the seam but subsonic compared with the wave velocity for the country rock is not treated here.)

The construction in Figure A.1 is purely geometrical and does not include the case of wave conversion at the boundaries between P and SV waves. The wave front can be taken as SH waves, for example. The dimensions are arbitrary, but the wave velocity in the homogeneous country rock is assumed to be much greater than that in the homogeneous seam. Refracted waves (D) would, by Huygen's principle, radiate in general from each point of the boundaries. In the country rock, the wave fronts (A') would move ahead of the corresponding fronts (A) in the seam; at the intersection of the front with the boundary there would be a conical head wave of diffracted type (shown as a dashed line D for the initial front only)

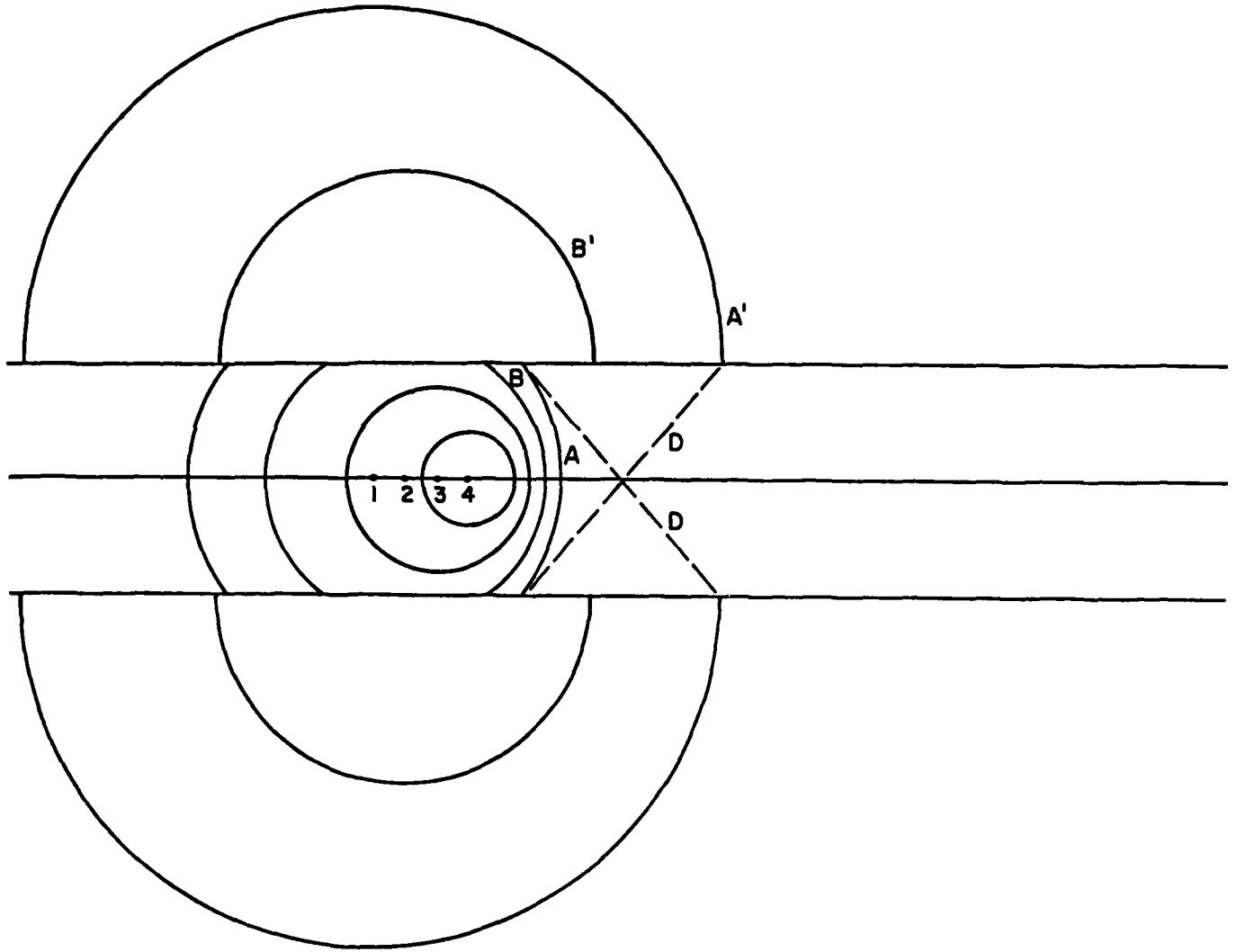

Figure A.1 Wave Fronts for a Moving Source in a Low-Velocity Channel

propagating in the seam as a leading fringe of energy.

A few inferences on the likely modifications to the effect of directivity focusing brought about by the seam can be drawn from Figure A.1:

(a) A simple quadrantal pattern with lobes would no longer describe the wave amplitudes in all the near field.

(b) The concentration of energy (focusing) in the forward direction is not as great just outside the seam as inside it. Shaking in the seam would commence before the arrival of the original initial pulse producing a longer duration and spreading of the wave energy.

(c) Enhanced damping of the waves in the seam would reduce the wave amplitudes there relative to waves refracted out of the seam.

(d) The diffraction, multiple reflection and progressive interference effects within the seam would be a function of the effective seam width relative to the wavelengths. In representative geological conditions, the higher frequency (above 5 Hz) waves are likely to be most attenuated by the multiple interference and damping within the seam.

APPENDIX B

DIRECTIVITY THEORY

Consider the effect of a finite moving source on the seismic surface wave radiation (Ben-Menahem, 1961). The solution for free surface radial Rayleigh wave displacements for a vertical strike-slip fault is

$$U_r^R = \frac{2 \cos \theta_o}{\sqrt{K_\beta r_o}} \; g_r(\omega) \left(\frac{\sin X_R}{X_R}\right) e^{i(\theta_R - \pi/4)} \qquad \text{(B.1)}$$

where

$$X_R = \frac{\omega b}{2c_R}\left(\frac{c_R}{V} - \cos \theta_o\right)$$

$$\phi_R = \omega\left(t - \frac{r_o}{c_R}\right) - X_R$$

θ_o = azimuthal angle on the free surface

K_β = shear wave number in half space

r_o = radial coordinate on the free surface

$g_r(\omega)$ = radial layering function for Rayleigh waves

b = dimension of fault in the direction of motion

ω = angular frequency

c_R = Rayleigh wave velocity

V = rupture velocity

r = time

The diffraction factor $\frac{\sin X_R}{X_R}$ in equation B.1 represents the finiteness

AD-A132 893 STATE-OF-THE-ART FOR ASSESSING EARTHQUAKE HAZARDS IN THE UNITED STATES RE..(U) CALIFORNIA UNIV BERKELEY B A BOLT AUG 83 WES-MP-S-73-1-20 DACW39-82-M-1125 2/2

UNCLASSIFIED F/G 8/11 NL

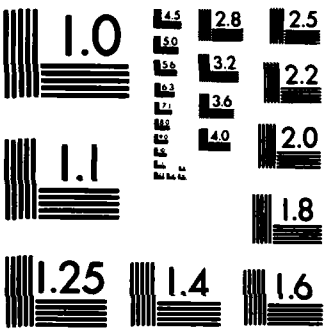

MICROCOPY RESOLUTION TEST CHART
NATIONAL BUREAU OF STANDARDS-1963-A

of the source in the direction of the propagating dislocation and its effect is to produce deviation from a purely dipole radiation pattern. This function produces nodes at

$$\frac{\omega b}{2c_R} \left(\frac{c_R}{V} - \cos \theta_o\right) = n\pi \quad \text{for } n = 1, 2, 3, \ldots \tag{B.2}$$

with the first node occurring at $2\pi/\omega = b\,[1/V - \cos \theta_o/c_R]$.

Rewrite equation B.2 as

$$\frac{b}{V} c_R - \cos \theta_o = n\lambda \tag{B.3}$$

where $\lambda = 2\pi V_R/\omega$.

This condition corresponds to destructive interference at the point of observation and is analogous to Fraunhofer diffraction through a rectangular slit. Note that as long as

$$n\pi < \left| \frac{\omega b}{2c_R} \left(\frac{c_R}{V} - \cos \theta_o\right) \right| < (n+1)\pi \tag{B.4}$$

no additional zeroes are introduced into the double-couple pattern and only a variation in amplitude is expected.

Now form the ratio of wave amplitudes at equal distances from the source in opposite directions, i.e.,

$$\frac{U_r^R(\theta_o)}{U_r^R(\pi+\theta_o)} = \frac{\dfrac{\sin \frac{\pi b}{\lambda}\left(\frac{c_R}{V} - \cos \theta_o\right)}{\frac{\pi b}{\lambda}\left(\frac{c_R}{V} - \cos \theta_o\right)}}{\dfrac{\sin \frac{\pi b}{\lambda}\left(\frac{c_R}{V} + \cos \theta_o\right)}{\frac{\pi b}{\lambda}\left(\frac{c_R}{V} + \cos \theta_o\right)}} \tag{B.5}$$

This ratio is the directivity function (Ben-Menahem, 1961). The function is independent of the source time function and is dependent only on the horizontal dimension of source, the velocity of rupture and the strike of fault with respect to the line joining the station with the epicenter. This function may have any value from zero to infinity. As (b/λ) decreases, it approaches unity and provides a measure for the horizontal dimension of source and the speed of rupture.

For a simple application, equation B.5 can be written as

$$D = \frac{(\frac{c}{V} + \cos\theta_o) \sin \frac{\pi b}{\lambda} (\frac{c}{V} - \cos\theta_o)}{(\frac{c}{V} - \cos\theta_o) \sin \frac{\pi b}{\lambda} (\frac{c}{V} + \cos\theta_o)} \qquad (B.6)$$

where c stands for either Rayleigh or Love phase velocity.

Both the directivity function (B.6) and the phase differential have now been used to estimate the length of fault rupture and the rupture velocity in quite a number of earthquakes. Source parameters are obtained from seismograms from two stations located at opposite ends of the fault or from surface waves of different order (R1, R2, ... etc.) recorded at a single station. If the waves travelling in opposite directions do not travel the same distance, the seismograms must be adjusted to equal seismic paths.

In one of the first successful regional studies for California earthquakes, spectral nodes for Love waves from the 1966 Parkfield earthquake observed at Berkeley, California (at a distance of 270 km) were used by Filson and McEvilly (1967) to infer its source parameters. Using the first node at T = 22.5 seconds, they estimated a rupture velocity of 2.2 km/sec.

REPORTS IN THIS SERIES
(MP S-73-1)

Report 1	O. W. Nuttli	Design Earthquakes for the Central United States	January 1973
Report 2	E. L. Krinitzsky	Fault Assessment in Earthquake Engineering	May 1974
Report 3	R. B. Hofmann	Factors in the Specification of Ground Motions for Design Earthquakes in California	June 1974
Report 4	Ellis L. Krinitzsky Frank K. Chang	Earthquake Intensity and the Selection of Ground Motion for Seismic Design	September 1975
Report 5	Jack L. Walper	Plate Tectonics and Earthquake Assessment	March 1976
Report 6	David B. Slemmons	Faults and Earthquake Magnitude	May 1977
Report 7	Ellis L. Krinitzsky Frank K. Chang	Specifying Peak Motions for Design Earthquakes	December 1977
Report 8	Frank K. Chang Ellis L. Krinitzsky	Duration, Spectral Content, and Predominant Period of Strong Motion Earthquake Records from Western United States	December 1977
Report 9	Frank K. Chang	Catalogue of Strong Motion Earthquake Records, Volume 1, Western United States, 1933-1971	April 1978
Report 10	Otto W. Nuttli John J. Dwyer	Attenuation of High-Frequency Seismic Waves in the Central Mississippi Valley	July 1978
Report 11	Charles E. Glass David B. Slemmons	Imagery in Earthquake Analysis	December 1978
Report 12	Otto W. Nuttli Robert B. Herrmann	Credible Earthquakes for the Central United States	December 1978
Report 13	M. K. Yegian	Probabilistic Seismic Hazard Analysis	July 1979
Report 14	Erik H. Vanmarcke	Representation of Earthquake Ground Motion: Scaled Accelerograms and Equivalent Response Spectra	August 1979
Report 15	James R. Houston	Tsunamis, Seiches, and Landslide-Induced Water Waves	November 1979
Report 16	Otto W. Nuttli	The Relation of Sustained Maximum Ground Acceleration and Velocity to Earthquake Intensity and Magnitude	November 1979
Report 17	Bruce A. Bolt	Interpretation of Strong Ground Motion Records	October 1981
Report 18	Daniele Veneziano	Errors in Probabilistic Seismic Hazard Analysis	January 1982
Report 19	Ronald B. Meade	The Evidence for Reservoir-Induced Macroearthquakes	June 1982
Report 20	Bruce A. Bolt	The Contribution of Directivity Focusing to Earthquake Intensities	August 1983

END

FILMED

10-83

DTIC